

Bianisotropic multi-layer analysis software - formulation and user guide

Q-par/AJM/anlay/1/v2.0



Q-par Angus Ltd
IDEAS ENGINEERED

Cover + vii + 68 pages

May 2011

Barons Cross Laboratories,
Leominster, Herefordshire, HR6 8RS, UK.
Tel: +44 (0) 1568 612138 Fax: +44 (0) 1568 616373
Web: www.q-par.com E-mail: sales@q-par.com



This document has been prepared by Q-par Angus Ltd., and may not be used or copied without proper authorisation.

© Copyright 2011
Q-par Angus Ltd., U.K.

Author	Q-par Angus Ltd.
Date	May 2011
Issued by	Q-par Angus Ltd. Barons Cross Laboratories Leominster Herefordshire HR6 HRS UK.

Document changes record

Issue	Date	Change summary
Issue 1.0	September 2010	First version
Issue 1.1	October 2010	Added remarks on general tensor forms
Issue 2.0	May 2011	Revised formulation and impedance surfaces

Abstract

This document describes the formulation of theory for the plane wave excitation of multi-layered structures containing bianisotropic materials and surface impedance sheets. It also provides a user guide for the software constructed around the method and examples showing its use. One example shows the design of a novel octave bandwidth linear-to-circular *reflector* polariser.

List of contents

Document changes record	iv
Abstract	v
List of contents	vi
List of figures	vii
1 Introduction	1
1.1 Scope of problem	1
1.2 Polarisation definitions and wave conventions	2
2 The formulation	5
2.1 The tensor constitutive relationships	5
2.2 Some dyadic and matrix notation for describing tensors	5
2.3 The transverse formulation method 1	8
2.4 The transverse formulation method 2	17
2.5 Energy measures and subsidiary quantities	33
2.6 Special types of materials	35
2.7 Surface impedance models	38
3 Software user guide	40
3.1 Introduction	40
3.2 Key word descriptions	41
3.3 Output file formats	46
3.4 Example 1. An anisotropic material for polarisation conversion in free space.	48
3.5 Example 2. An anisotropic radome composite in free space.	51
3.6 Example 3. A bianisotropic material in free space.	54
3.7 Example 4. An anisotropic RAM.	57
3.8 Example 5. A new kind of reflection polariser.	60
3.9 Example 6. A sheet polariser showing the problem with formulation 1	62
3.10 Example 7. Optimised 4-sheet polarisers using formulation 2.	64
4 References	68

List of figures

1-1	Plane wave excitation of a multiple layer structure	2
2-1	A structure consisting of $N - 1$ layers (shown as a free structure)	10
2-2	A structure consisting of N layers with impedance surfaces between layers.	17
2-3	The general canonical structure associated with layer i .	25
2-4	The special canonical structure associated with the first interface.	27
2-5	The special canonical structure referring to layer terminated by a perfect conductor.	28
2-6	Concatenation of partial structure with the next layer.	30
2-7	Equivalent circuit models for the principal surface admittances	39
3-1	Output powers and axial ratio for a y-polarised incident wave	50
3-2	Co-polar Transmission for incident TE waves	53
3-3	Co-polar Transmission for incident TM waves	53
3-4	Transmittance T_{TE} for incident TE waves (linear scale)	56
3-5	Transmittance T_{TM} for incident TE waves (linear scale)	56
3-6	Co-polar Reflection for incident TE waves	59
3-7	Co-polar Reflection for incident TM waves	59
3-8	An ABA/2 PEC terminated structure for the design of a reflector polariser (linear to circular)	60
3-9	Output powers and axial ratio for a y-polarised incident wave	61
3-10	Transmission coefficients for a 45 degree polariser using software version 00.02.00 and ill-conditioning (formulation 1).	63
3-11	Transmission coefficients for a 45 degree polariser using software version 00.03.02 and no ill-conditioning (formulation 2).	63
3-12	Reflection coefficients $\mathcal{R}_{11}, \mathcal{R}_{12}, \mathcal{R}_{21}, \mathcal{R}_{22}$ in dB for example 7a.	66
3-13	Transmission coefficients $\mathcal{T}_{11}, \mathcal{T}_{12}, \mathcal{T}_{21}, \mathcal{T}_{22}$ in dB for example 7a.	66
3-14	Reflection coefficients $\mathcal{R}_{11}, \mathcal{R}_{12}, \mathcal{R}_{21}, \mathcal{R}_{22}$ in dB for example 7b.	67
3-15	Transmission coefficients $\mathcal{T}_{11}, \mathcal{T}_{12}, \mathcal{T}_{21}, \mathcal{T}_{22}$ in dB for example 7b.	67

1 Introduction

1.1 Scope of problem

There is an increasing use of artificial dielectrics and metamaterials intended for multiple applications in antenna engineering. Any material which is uniform on one scale but shows structure on a smaller (typically, but not always, sub-wavelength) scale can be regarded as such. These can often be modelled as linear and passive, but where the constitutive relations relating the magnetic \underline{B} and \underline{H} fields and electric \underline{D} and \underline{E} fields are tensors.

Many materials exist in nature which require anisotropic tensor relations, especially at optical frequencies, but many have been synthesised artificially which have no known natural analogues. It is of importance to be able to analyse these materials and to determine the transmission and reflection characteristics. Applications include the design of filters, polarisers (linear to circular, linear to linear, etc.) and as backings for antenna arrays.

This analysis assumes a layered material with an arbitrary number of layers each composed of a general bianisotropic material. Each layer is assumed infinite in lateral extent with finite specified thickness. The material is assumed to be impinged upon by a plane wave of arbitrary polarisation and angle of incidence. The structure may be *open* with free space on either side or backed by a perfect conductor. In this case its electromagnetic properties are specified by a single reflection and transmission matrix from which other auxiliary parameters (such as absorbed energy, degree of depolarisation, axial ratio etc.) can be determined.

We update the original Rikte formulation to provide a method which is substantially well conditioned for arbitrary materials of arbitrary thickness and also allows the option of placing thin impedance sheets (e.g. frequency selective surfaces or polarising grids) between layers.

We will assume that each layer is infinite in the x-y plane and transverse to the z-direction. An incident plane wave is specified with incidence angles (θ_{in}, ϕ_{in}) , and the transmitted and reflected waves by the angles, (θ_{tx}, ϕ_{tx}) and (θ_{rx}, ϕ_{rx}) , respectively. Figure 1-1 indicates such a structure and the coordinate system associated with it.

It is important to note that the Cartesian (x, y, z) coordinate system employed is a *global* one. Under this, and using Snell's law, we have

$$\begin{aligned}\theta_{tx} &= \theta_{in} & \phi_{tx} &= \phi_{in} \\ \theta_{rx} &= \pi - \theta_{in} & \phi_{rx} &= \phi_{in}\end{aligned}\tag{1-1}$$

assuming the wave is always described pointing in the same direction (towards the origin) with respect to the coordinate system. We term this the *with-the-wave* coordinate system, and its use has some subtle consequences that will be described later. This coordinate system is also the one employed by us in [2].

The main analysis in this report is taken from Rikte et al. [1] with some modifications (see later), principally concerned with evaluation of matrix exponentials and in the definition of output quantities. The reader is strongly advised to read [1] for more detailed explanation of certain points.

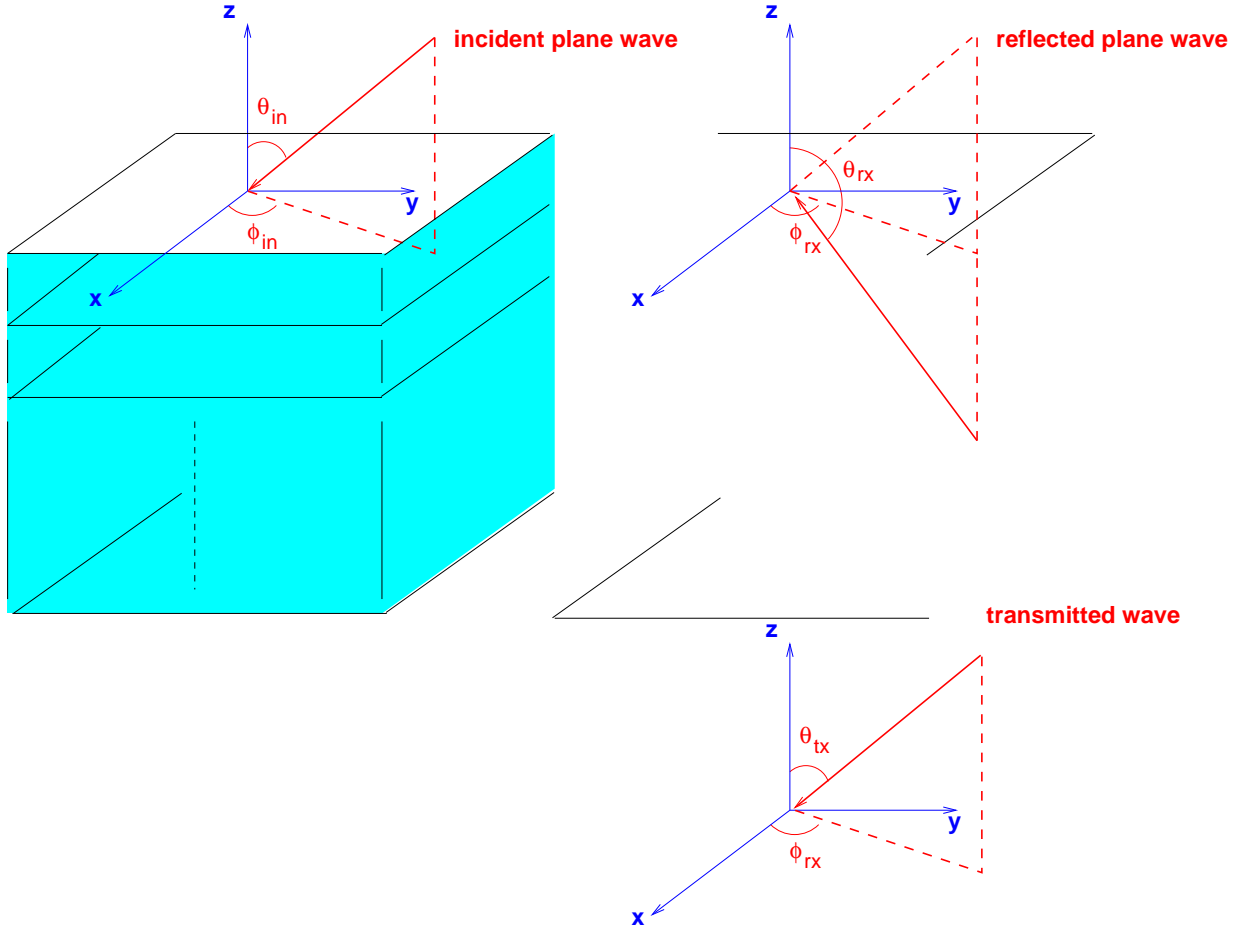


Figure 1-1: Plane wave excitation of a multiple layer structure

1.2 Polarisation definitions and wave conventions

We assume, throughout this report, a harmonic time dependence $e^{j\omega t}$ where $\omega = 2\pi f$ is the angular frequency and f is the frequency in Hz.¹ This implies, for an isotropic material with scalar relative permittivity and scalar relative permeability ϵ_r and μ_r , that ϵ_r and μ_r have zero or negative imaginary parts if the material is passive and lossy. Similar requirements, suitably generalised, may be made of the relative permittivity and permeability tensors for an anisotropic material (see later).

¹In Rikte et al. [1] the alternative $e^{-i\omega t}$ time convention is employed. Thus their i should be replaced, whenever it occurs, by $-j$ in our formulation. We employ the j notation for consistency with [2] as is common in electrical engineering (rather than in physics and mathematics).

A plane wave is defined in two transverse coordinate systems; in terms of the unit vectors $\underline{\hat{x}}$ and $\underline{\hat{y}}$, and in terms of the unit vectors $\underline{\hat{e}}_{\parallel}(\phi)$ (parallel) and $\underline{\hat{e}}_{\perp}(\phi)$ (perpendicular) at an angle ϕ to the x-axis in the x-y plane. This follows Rikte et al. notation with,

$$\begin{aligned}\underline{\hat{e}}_{\parallel}(\phi) &= \underline{\hat{x}} \cos \phi + \underline{\hat{y}} \sin \phi \\ \underline{\hat{e}}_{\perp}(\phi) &= -\underline{\hat{x}} \sin \phi + \underline{\hat{y}} \cos \phi\end{aligned}\tag{1-2}$$

and we will abbreviate

$$\begin{aligned}\underline{\hat{e}}_{\parallel} &\equiv \underline{\hat{e}}_{\parallel}(\phi_{in}) \\ \underline{\hat{e}}_{\perp} &\equiv \underline{\hat{e}}_{\perp}(\phi_{in})\end{aligned}\tag{1-3}$$

because it turns out that we only need these vectors evaluated when $\phi = \phi_{in}$.

The unit vectors (1-3) are the unit projections of $\underline{\hat{\theta}}_{in}$ and $\underline{\hat{\phi}}_{in}$ where,

$$\begin{aligned}\underline{\hat{\theta}}_{in} &= \cos \theta_{in} \underline{\hat{e}}_{\parallel} - \sin \theta_{in} \underline{\hat{z}} \\ \underline{\hat{\phi}}_{in} &= \underline{\hat{e}}_{\perp}\end{aligned}\tag{1-4}$$

We may similarly define unit vectors associated with the transmitted and reflected waves,

$$\begin{aligned}\underline{\hat{\theta}}_{tx} &= \underline{\hat{\theta}}_{in} \\ \underline{\hat{\phi}}_{tx} &= \underline{\hat{\phi}}_{in}\end{aligned}\tag{1-5}$$

and

$$\begin{aligned}\underline{\hat{\theta}}_{rx} &= -\cos \theta_{in} \underline{\hat{e}}_{\parallel} - \sin \theta_{in} \underline{\hat{z}} \\ \underline{\hat{\phi}}_{rx} &= \underline{\hat{\phi}}_{in}\end{aligned}\tag{1-6}$$

Note the negative sign on the $\underline{\hat{e}}_{\parallel}$ term for $\underline{\hat{\theta}}_{rx}$ due to the angle change in (1-1).

If the projection of a wave vector onto the x-y plane lies in the $\underline{\hat{e}}_{\parallel}$ direction it is a $\underline{\hat{\theta}}$ -directed transverse magnetic (TM) wave. If the projection of a wave vector onto the x-y plane lies in the $\underline{\hat{e}}_{\perp}$ direction it is a $\underline{\hat{\phi}}$ -directed transverse electric (TE) wave.²

When $\theta_{in} = 0$ a wave is both TE and TM or TEM. This needs no special case, however, since both $\underline{\hat{e}}_{\parallel}$ and $\underline{\hat{e}}_{\perp}$ are well defined here.

An incident wave pointing towards the origin has a vector wave number,

$$\underline{k}_{in} = \underline{k}_t + \underline{\hat{z}}k_z\tag{1-7}$$

²The parallel/perpendicular nomenclature can be confusing since some authors refer to the parallel wave as one in which the E-field lies parallel (in the plane) of the material, i.e. in the $\underline{\hat{\phi}}$ direction, which is the reverse of the definition used here.

where the transverse component,

$$\begin{aligned}\underline{k}_t &= -k_0 \sin \theta_{in} \hat{e}_{||} \\ k_z &= -k_0 \cos \theta_{in}\end{aligned}\quad (1-8)$$

where k_0 is the free space wave number $k_0 = 2\pi/\lambda_0 = \omega/c_0$ with λ_0 as the free space wavelength and c_0 the speed of light in vacuum. $\hat{\underline{\theta}}_{in}$, $\hat{\underline{\phi}}_{in}$ and $\underline{k}_{in}/|\underline{k}_{in}|$ form the with-the-wave orthonormal coordinate system for the incident wave.

The electric field vector amplitudes associated with the incident, transmitted and reflected waves may be defined by,

$$\begin{aligned}\underline{E}_{in} &= \alpha_{in}^{(\phi)} \hat{\underline{\phi}}_{in} + \alpha_{in}^{(\theta)} \hat{\underline{\theta}}_{in} \\ \underline{E}_{tx} &= \alpha_{tx}^{(\phi)} \hat{\underline{\phi}}_{tx} + \alpha_{tx}^{(\theta)} \hat{\underline{\theta}}_{tx} \\ \underline{E}_{rx} &= \alpha_{rx}^{(\phi)} \hat{\underline{\phi}}_{rx} + \alpha_{rx}^{(\theta)} \hat{\underline{\theta}}_{rx}\end{aligned}\quad (1-9)$$

where the α coefficients are (in general) complex scalars. The principal required outputs from the formulation are the reflectance and transmittance matrices that relate the α coefficients. We define these by,

$$\mathcal{T} = \begin{pmatrix} \mathcal{T}_{\perp\perp} & \mathcal{T}_{\parallel\perp} \\ \mathcal{T}_{\perp\parallel} & \mathcal{T}_{\parallel\parallel} \end{pmatrix} \equiv \begin{pmatrix} \mathcal{T}_{11} & \mathcal{T}_{12} \\ \mathcal{T}_{21} & \mathcal{T}_{22} \end{pmatrix}\quad (1-10)$$

and

$$\mathcal{R} = \begin{pmatrix} \mathcal{R}_{\perp\perp} & \mathcal{R}_{\parallel\perp} \\ \mathcal{R}_{\perp\parallel} & \mathcal{R}_{\parallel\parallel} \end{pmatrix} \equiv \begin{pmatrix} \mathcal{R}_{11} & \mathcal{R}_{12} \\ \mathcal{R}_{21} & \mathcal{R}_{22} \end{pmatrix}\quad (1-11)$$

where

$$\begin{bmatrix} \alpha_{tx}^{(\phi)} \\ \alpha_{tx}^{(\theta)} \end{bmatrix} = \mathcal{T}^T \begin{bmatrix} \alpha_{in}^{(\phi)} \\ \alpha_{in}^{(\theta)} \end{bmatrix}\quad (1-12)$$

and

$$\begin{bmatrix} \alpha_{rx}^{(\phi)} \\ \alpha_{rx}^{(\theta)} \end{bmatrix} = \mathcal{R}^T \begin{bmatrix} \alpha_{in}^{(\phi)} \\ \alpha_{in}^{(\theta)} \end{bmatrix}\quad (1-13)$$

where the ‘ T ’ superscript represents the matrix transpose. The matrix transpose is employed to permit the same definitions of \mathcal{T} and \mathcal{R} as are used in [2]³

³Rikte et al. [1] do not explicitly employ these matrices in their formulation.

2 The formulation

2.1 The tensor constitutive relationships

At a given frequency, the Maxwell equations relating \underline{D} , \underline{E} , \underline{B} and \underline{H} fields are,

$$\begin{aligned}\nabla \times \underline{E} &= -jk_0c_0\underline{B} \\ \nabla \times (\eta_0\underline{H}) &= +jk_0c_0\eta_0\underline{D}\end{aligned}\tag{2-1}$$

If materials are assumed to be linear then the most general constitutive relationship between the fields is given by,

$$\begin{aligned}\underline{D} &= \epsilon_0(\underline{\xi} \cdot \underline{E} + \eta_0 \underline{\xi} \cdot \underline{H}) \\ \underline{B} &= \frac{1}{c_0}(\underline{\zeta} \cdot \underline{E} + \eta_0 \underline{\mu} \cdot \underline{H})\end{aligned}\tag{2-2}$$

where $\underline{\xi}$ is the relative permittivity tensor, $\underline{\mu}$ is the relative permeability tensor and $\underline{\xi}$ and $\underline{\zeta}$ are respectively the xi and zeta chirality tensors. These tensors are dimensionless and may be expressed as 3×3 matrices. ϵ_0 is the permittivity of free space ($\approx 8.854 \times 10^{-12}$ F/m in SI units), $\eta_0 = \sqrt{\mu_0/\epsilon_0}$ is the impedance of free space (≈ 376.7 ohms) and μ_0 is the permeability of free space ($= 4\pi \times 10^{-7}$ H/m in SI units).

We will make no assumptions about the realisability of permitted dispersion relationships; i.e. the nature of the frequency dependence of each of these tensors for physically realisable materials. This is still a research topic and only limited results are available.

For most applications, the full generality expressed in (2-2) is not required and some special cases are of use (and are employed) in describing inputs to the software implementation. These are described in section 2.6 below. However, before proceeding further some (slightly non-standard) notation is required.

2.2 Some dyadic and matrix notation for describing tensors

Rikte et al [1] employ dyadic notations for tensor algebra. We have expanded on this slightly to avoid confusion on the dimension of various quantities.

Firstly, all second order tensors can be expressed by square matrices in a specified coordinate base with certain transformation properties. Depending on context, these matrices and the matrices that operate on them may be either 2×2 or 3×3 depending on whether they are employed to represent full-component or transverse component fields. Except where specifically noted, we employ a Cartesian x-y-z coordinate base. Similarly vectors may be either of dimension 3 or dimension 2. Where there is possible confusion, we will use the superscript (n) to represent an n-dimensional quantity. In this report n may be 2, 3 or 4.

There are two basic tensor operations; an outer and an inner product. The outer product of two 3-dimensional vectors is the matrix defined by,

$$\underline{a} \underline{b} \equiv \underline{a}^{(3)} \underline{b}^{(3)} = \begin{pmatrix} a_1 \\ a_2 \\ a_3 \end{pmatrix} (b_1 \ b_2 \ b_3) = \begin{pmatrix} a_1 b_1 & a_1 b_2 & a_1 b_3 \\ a_2 b_1 & a_2 b_2 & a_2 b_3 \\ a_3 b_1 & a_3 b_2 & a_3 b_3 \end{pmatrix} \quad (2-3)$$

The inner product of two 3-dimensional vectors is the usual dot product,

$$\underline{a} \cdot \underline{b} = a_1 b_1 + a_2 b_2 + a_3 b_3 \quad (2-4)$$

We do not require the outer product of matrices or the outer product of a matrix with a vector so these are not defined here. The inner product of two matrices is the standard matrix-matrix multiplication and will be given no special notation. The inner product of a matrix with a vector depends on the order of operation as,

$$\underline{\underline{A}} \cdot \underline{b} \equiv \mathbf{A} \mathbf{b} = \begin{pmatrix} A_{11} & A_{12} & A_{13} \\ A_{21} & A_{22} & A_{23} \\ A_{31} & A_{32} & A_{33} \end{pmatrix} \begin{pmatrix} b_1 \\ b_2 \\ b_3 \end{pmatrix} \quad (2-5)$$

or

$$\underline{b} \cdot \underline{\underline{A}} \equiv \mathbf{b}^T \mathbf{A} = (\mathbf{A}^T \mathbf{b})^T = (b_1 \ b_2 \ b_3) \begin{pmatrix} A_{11} & A_{12} & A_{13} \\ A_{21} & A_{22} & A_{23} \\ A_{31} & A_{32} & A_{33} \end{pmatrix} \quad (2-6)$$

Using this notation we have a tensor decomposition,

$$\underline{\underline{A}}^{(3)} = \underline{\underline{A}}_{\perp\perp}^{(3)} + \hat{\underline{\underline{z}}} \underline{\underline{A}}_z^{(3)} + \underline{\underline{A}}_{\perp}^{(3)} \hat{\underline{\underline{z}}} + A_{zz} \hat{\underline{\underline{z}}} \hat{\underline{\underline{z}}} \quad (2-7)$$

In a Cartesian coordinate base, such that the matrix $\underline{\underline{A}}$ transforms between the Cartesian vectors (x_1, y_1, z_1) and (x_2, y_2, z_2) ,

$$\begin{pmatrix} x_2 \\ y_2 \\ z_2 \end{pmatrix} = \begin{pmatrix} A_{11} & A_{12} & A_{13} \\ A_{21} & A_{22} & A_{23} \\ A_{31} & A_{32} & A_{33} \end{pmatrix} \begin{pmatrix} x_1 \\ y_1 \\ z_1 \end{pmatrix} \quad (2-8)$$

then we have

$$\underline{\underline{A}}_{\perp\perp}^{(3)} = \begin{pmatrix} A_{11} & A_{12} & 0 \\ A_{21} & A_{22} & 0 \\ 0 & 0 & 0 \end{pmatrix} \equiv \begin{pmatrix} \underline{\underline{A}}_{\perp\perp}^{(2)} & 0 \\ 0 & 0 \end{pmatrix} \quad (2-9)$$

the vectors,

$$\underline{\underline{A}}_z^{(3)} = (A_{31} \ A_{32} \ 0) \equiv (\underline{\underline{A}}_z^{(2)} \ 0) \quad (2-10)$$

$$\underline{\underline{A}}_{\perp}^{(3)} = \begin{pmatrix} A_{13} \\ A_{23} \\ 0 \end{pmatrix} = \begin{pmatrix} \underline{\underline{A}}_{\perp}^{(2)} \\ 0 \end{pmatrix} \quad (2-11)$$

and the scalar,

$$A_{zz} = A_{33} \quad (2-12)$$

This decomposition is applied to $\underline{\underline{\epsilon}}$, $\underline{\underline{\mu}}$, $\underline{\underline{\zeta}}$ and $\underline{\underline{\xi}}$.

We also follow Rikte et al. [1] in defining the 3×3 and 2×2 unit matrices as,

$$\underline{\underline{I}}_3 \equiv \underline{\underline{I}}_3^{(3)} = \begin{pmatrix} 1 & 0 & 0 \\ 0 & 1 & 0 \\ 0 & 0 & 1 \end{pmatrix} \quad (2-13)$$

$$\boldsymbol{I} \equiv \underline{\underline{I}}_2 \equiv \underline{\underline{I}}_2^{(2)} = \begin{pmatrix} 1 & 0 \\ 0 & 1 \end{pmatrix} \quad (2-14)$$

and the rotation matrix,

$$\boldsymbol{J} \equiv \underline{\underline{J}} \equiv \underline{\underline{J}}_2 \equiv \underline{\underline{J}}_2^{(2)} = \begin{pmatrix} 0 & 1 \\ -1 & 0 \end{pmatrix} \quad (2-15)$$

with the various notations depending on context. Note that we will use bold type face to represent 2×2 matrices, rather than the dyadic double-underline notation, when there is little chance of confusion.

2.3 The transverse formulation method 1

2.3.1 Introduction to method 1

In this section we provide a derivation, with expanded comments, of Rikte's method [1]. This forms the basis of our first software implementation (up to and including software version 00.01.005). However, as we point out, there are certain numerical conditioning problems associated with this method. These are not usually serious if we do *not* generalise the method to include thin sheets (such as polarising grids) or certain types of frequency selective surfaces (FSS) between layers.

However, we will wish to generalise the method to include such thin sheets and also make the method more stable when employing absorbent materials. To this end we will also detail a second (novel) formulation in section 2.4 which will form the basis of software version 00.03.00+.

The first subsection, section 2.3.2, describes formulation elements which are common to all our transverse methods. Section 2.3.3 outlines Rikte's basic concatenation method with no thin sheets between layers. Section 2.3.4 describes the derivation of the reflection and transmission coefficient matrices employing the above concatenation method. Some of the terms defined here will be employed in later formulations, but it is essentially descriptive of method 1. Section 2.3.5 derives the reflectance and transmittance matrices given the tangential reflection and transmission matrices. This section is common to all methods.

2.3.2 Common formulation elements

Within a homogeneous region, i.e. within one of the layers of a layered material, Maxwell's equations can be written in terms only of the transverse field components. If we write the x and y components of the field as the 2-component column vectors,

$$\begin{aligned}\underline{E}_{xy} &\equiv \underline{E}_{xy}^{(2)} = (E_x, E_y)^T \\ \underline{H}_{xy} &\equiv \underline{H}_{xy}^{(2)} = (H_x, H_y)^T\end{aligned}\tag{2-16}$$

then it can be shown [1] that,

$$\frac{d}{dz} \begin{pmatrix} \underline{E}_{xy}(z) \\ \eta_0 \underline{J}_2 \cdot \underline{H}_{xy}(z) \end{pmatrix} = -jk_0 \underline{\underline{M}}^{(4)} \cdot \begin{pmatrix} \underline{E}_{xy}(z) \\ \eta_0 \underline{J}_2 \cdot \underline{H}_{xy}(z) \end{pmatrix}\tag{2-17}$$

where $\underline{\underline{M}} \equiv \underline{\underline{M}}^{(4)}$ is a 4-dimensional matrix containing terms of the relative permittivity, permeability and chirality tensors as defined in appendix C of [1]. For a general bianisotropic medium,

$$\underline{\underline{M}} = \begin{pmatrix} \mathbf{M}_{11} & \mathbf{M}_{12} \\ \mathbf{M}_{21} & \mathbf{M}_{22} \end{pmatrix}\tag{2-18}$$

where the 2×2 block matrix elements are given by,

$$\begin{aligned} \mathbf{M}_{11} = & -\underline{\underline{J}} \cdot \underline{\underline{\zeta}}_{\perp\perp}^{(2)} + a(\underline{k}_t/k_0 - \underline{\underline{J}} \cdot \underline{\underline{\zeta}}_{\perp}^{(2)})(-\mu_{zz}\epsilon_z^{(2)} - \xi_{zz}\underline{\underline{J}} \cdot \underline{k}_t/k_0 + \xi_{zz}\zeta_z^{(2)}) \\ & - a(\underline{\underline{J}} \cdot \underline{\underline{\mu}}_{\perp}^{(2)})(\zeta_{zz}\epsilon_z^{(2)} + \epsilon_{zz}\underline{\underline{J}} \cdot \underline{k}_t/k_0 - \epsilon_{zz}\zeta_z^{(2)}) \end{aligned} \quad (2-19)$$

$$\begin{aligned} \mathbf{M}_{12} = & \underline{\underline{J}} \cdot \underline{\underline{\mu}}_{\perp\perp}^{(2)} \cdot \underline{\underline{J}} + a(\underline{k}_t/k_0 - \underline{\underline{J}} \cdot \underline{\underline{\zeta}}_{\perp}^{(2)})(\mu_{zz}\underline{k}_t/k_0 + \mu_{zz}\xi_z^{(2)} \cdot \underline{\underline{J}} - \xi_{zz}\underline{\underline{\mu}}_z^{(2)} \cdot \underline{\underline{J}}) \\ & - a(\underline{\underline{J}} \cdot \underline{\underline{\mu}}_{\perp}^{(2)})(-\zeta_{zz}\underline{k}_t/k_0 - \zeta_{zz}\xi_z^{(2)} \cdot \underline{\underline{J}} + \epsilon_{zz}\underline{\underline{\mu}}_z^{(2)} \cdot \underline{\underline{J}}) \end{aligned} \quad (2-20)$$

$$\begin{aligned} \mathbf{M}_{21} = & -\underline{\underline{\epsilon}}_{\perp\perp}^{(2)} - a\underline{\underline{\epsilon}}_{\perp}^{(2)}(-\mu_{zz}\epsilon_z^{(2)} - \xi_{zz}\underline{\underline{J}} \cdot \underline{k}_t/k_0 + \xi_{zz}\zeta_z^{(2)}) \\ & + a(\underline{\underline{J}} \cdot \underline{k}_t/k_0 - \underline{\underline{\zeta}}_{\perp}^{(2)})(\zeta_{zz}\epsilon_z^{(2)} + \epsilon_{zz}\underline{\underline{J}} \cdot \underline{k}_t/k_0 - \epsilon_{zz}\zeta_z^{(2)}) \end{aligned} \quad (2-21)$$

$$\begin{aligned} \mathbf{M}_{22} = & \underline{\underline{\xi}}_{\perp\perp} \cdot \underline{\underline{J}} - a\underline{\underline{\epsilon}}_{\perp}^{(2)}(\mu_{zz}\underline{k}_t/k_0 + \mu_{zz}\xi_z^{(2)} \cdot \underline{\underline{J}} - \xi_{zz}\underline{\underline{\mu}}_z^{(2)} \cdot \underline{\underline{J}}) \\ & + a(\underline{\underline{J}} \cdot \underline{k}_t/k_0 - \underline{\underline{\xi}}_{\perp}^{(2)})(-\zeta_{zz}\underline{k}_t/k_0 - \zeta_{zz}\xi_z^{(2)} \cdot \underline{\underline{J}} + \epsilon_{zz}\underline{\underline{\mu}}_z^{(2)} \cdot \underline{\underline{J}}) \end{aligned} \quad (2-22)$$

where

$$a = \frac{1}{\epsilon_{zz}\mu_{zz} - \xi_{zz}\zeta_{zz}} \quad (2-23)$$

The case where $a \rightarrow \infty$ is a theoretical possibility within the formulation for which we take no special care. Currently, the software will terminate with an appropriate warning if a is excessively large. This is one of several special cases where the algorithm is currently ill-conditioned, but where there is unlikely to be a problem for realistic materials.

The expressions clearly take simpler forms under the special cases where the materials are isotropic, bi-isotropic or anisotropic. Expressions in these special cases are given in [1] and have been implemented for diagnostic purposes within the software⁴.

Solution of (2-17) within a single layer is given by,

$$\begin{pmatrix} \underline{E}_{xy}(z) \\ \eta_0 \underline{\underline{J}}_2 \cdot \underline{H}_{xy}(z) \end{pmatrix} = \underline{\underline{P}}^{(4)}(z, z_1) \cdot \begin{pmatrix} \underline{E}_{xy}(z_1) \\ \eta_0 \underline{\underline{J}}_2 \cdot \underline{H}_{xy}(z_1) \end{pmatrix} \quad (2-24)$$

where $\underline{\underline{P}}^{(4)}$ is the matrix exponential,

$$\underline{\underline{P}}^{(4)}(z, z_1) = \exp(-jk_0(z - z_1)\underline{\underline{M}}^{(4)}) \quad (2-25)$$

⁴It is not required to use the special cases within the software *except* to make diagnostic checks, so the routines for special purpose construction are generally commented out in the source code.

where z and z_1 lie in the same homogeneous region. Accurate computation of general matrix exponentials is surprisingly difficult and is still a research topic in mathematics. Generally there should be no problem if the matrix to be exponentiated is well conditioned in the sense of a *normal matrix*, but this may not always be the case for certain kinds of realisable materials. In particular, the Cayley-Hamilton method described (and presumably employed) in [1] will fail when the eigenvalues of $\underline{\underline{M}}$ coalesce. This will occur for nearly isotropic materials (which are normal matrix well conditioned) and for ‘Tellegen’ materials (which may not be normal matrix well conditioned).

As of the year 2003, the state of the art concerning matrix exponentiation is given by Moler and Loan [3]. For small order dense general complex matrices (such as $\underline{\underline{M}}$) it would seem that the best algorithm is one employed (and with freely available source code) in the *Expokit* software suite [4]. We employ the routine **zgpadm** which uses a variant of the scaling and squaring method.⁵

2.3.3 Basic formulation with no surface discontinuities

If there are no surface discontinuities, i.e. no thin material sheets or frequency selective surfaces between layers, then the fields \underline{E}_{xy} and \underline{H}_{xy} are both continuous across the boundary between layers and the general solution to the fields across a multiple layer structure can be concatenated as the product of the solution to a single layer as presented in [1].

Suppose a structure consisting of $N - 1$ layers (N interfaces) with a wave incident in medium 1 and transmitted (for a free structure) in material N as shown in figure 2-1. The tangential

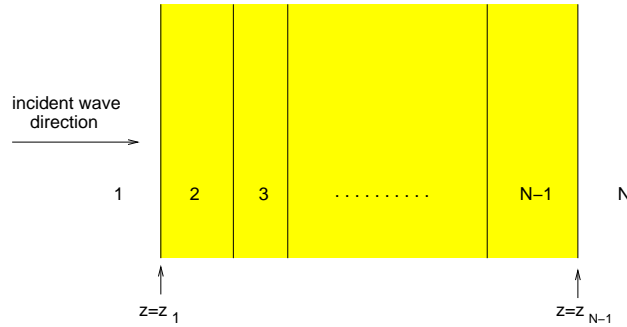


Figure 2-1: A structure consisting of $N - 1$ layers (shown as a free structure)

fields at the first interface, where $z = z_1$, are related using (2-24) to the tangential fields at the final interface, where $z = z_{N-1}$, by

$$\begin{pmatrix} \underline{E}_{xy}(z_{N-1}) \\ \eta_0 \underline{J}_2 \cdot \underline{H}_{xy}(z_{N-1}) \end{pmatrix} = \underline{\underline{P}}^{(4)}(z_{N-1}, z_1) \cdot \begin{pmatrix} \underline{E}_{xy}(z_1) \\ \eta_0 \underline{J}_2 \cdot \underline{H}_{xy}(z_1) \end{pmatrix} \quad (2-26)$$

⁵Software may now exist with better (more accurate, more robust and/or more efficient) algorithms, especially given the seven years since the publication of [3], but we have been unable to find any such non-commercial software. Experiments to date have found *zgpadm* to be quite sufficient for our application.

where

$$\begin{aligned} \underline{\underline{P}}^{(4)}(z_{N-1}, z_1) = & \exp(-jk_0(z_{N-1} - z_{N-2})\underline{\underline{M}}_{N-1}^{(4)}) \\ & \exp(-jk_0(z_{N-2} - z_{N-3})\underline{\underline{M}}_{N-2}^{(4)}) \dots \exp(-jk_0(z_2 - z_1)\underline{\underline{M}}_2^{(4)}) \end{aligned} \quad (2-27)$$

Note that equation (2-27) involves the product of matrix exponentials. In general this *cannot* be written as the matrix exponential of the sum of the arguments since for non-normal matrices $\exp \underline{\underline{A}} \cdot \exp \underline{\underline{B}} \neq \exp(\underline{\underline{A}} + \underline{\underline{B}})$.

This formulation, as used by [1], is relatively straight forward but is not always well conditioned. The problem lies with the fact that in general $\underline{\underline{P}}^{(4)}(z_{N-1}, z_1)$ involves both exponentially large as well as exponentially small terms under certain realisable conditions. This includes where one or many of the layers are very lossy. When relating the transmitted and reflected waves to the tangential fields at the interfaces z_1 and z_{N-1} these large terms are algebraically removed, as may be seen below, but the formulation can be ill-conditioned when cancellations are required in the differences of large numbers. The problem is mentioned in [1], but not solved.

The solution would appear to be difficult since it involves “wave splitting” within the general bianisotropic material of each layer in terms of forward and backward propagating wave modes. While formally this is possible (and the method for doing this is given in appendix D of [1]) in practice it is hard. Such a method requires the eigen decomposition of each of the matrices $\underline{\underline{M}}_i$ for each layer, prior to matrix exponentiation. The determination of eigenvectors and eigenvalues is not a problem and actually provides a simple means of matrix exponentiation, but only when the eigenvalues are distinct and the matrices $\underline{\underline{M}}_i$ are normal matrices. The problem occurs when this is not or nearly not the case, when we need to treat all possible special cases of matrix exponentiation in a well conditioned manner. The mathematical problems are addressed in [3].

Physically, there are certain conditions for which it is known that a non-uniaxial (biaxial) lossless material can give rise to degenerate wave directions in the material. An example of this is the *conical refraction* effect where there is a cone of permitted wave directions in the material for a given incident wave.

For many examples, where materials are not very lossy or (as is the case in this section) we are not coupling FSS interfaces with strong evanescent fields through such media, the numerical ill-conditioning appears to be rarely problematic and was not an issue in the examples presented in [1] and duplicated later in this report. However if software, such as formulated for QDAS [2], were to employ such materials it is necessary to solve this problem. One (but not the only) consequence of such ill conditioning is for the appearance of large numbers in $\underline{\underline{P}}^{(4)}(z_{N-1}, z_1)$. Some tests and diagnostics are included within the software to check for such problems, but ill conditioning can also manifest by a successive degradation in accuracy resulting in poor condition numbers for certain matrix inverses required in the next section.

2.3.4 Determination of the tangential reflection and transmission matrices

In this section we employ the same formulation as given [1] but derive the results in a different manner. Other than to provide confirmation we believe it provides a slightly more intuitive picture in terms of TE and TM plane wave components. Firstly, any plane wave in free space satisfies the relation between E and H fields given by,

$$\underline{E} = -\eta_0 \hat{k} \times \underline{H} \quad (2-28)$$

Expressing the vector fields as the sum of transverse and z-directed components,

$$\begin{aligned} \underline{E} &= \underline{E}^t + E_z \hat{z} \\ \underline{H} &= \underline{H}^t + H_z \hat{z} \\ \hat{k} &= (\underline{k}^t + k_z \hat{z})/k_0 \end{aligned} \quad (2-29)$$

together with the other properties of a plane wave,

$$\begin{aligned} \underline{k} \cdot \underline{H} &= 0 \\ \underline{k} \cdot \underline{E} &= 0 \end{aligned} \quad (2-30)$$

$$(2-31)$$

we obtain,

$$\left(\underline{E}^t - \frac{\underline{k}^t \cdot \underline{E}^t}{k_z} \hat{z} \right) = -\frac{\eta_0}{k_0} (\underline{k}^t + k_z \hat{z}) \times \left(\underline{H}^t - \frac{\underline{k}^t \cdot \underline{H}^t}{k_z} \hat{z} \right) \quad (2-32)$$

from which we obtain the expression relating tangential components,

$$\underline{E}^t = -\frac{\eta_0}{k_0} \left(k_z \hat{z} \times \underline{H}^t - \frac{\underline{k}^t \cdot \underline{H}^t}{k_z} \underline{k}^t \times \hat{z} \right) \quad (2-33)$$

If the plane wave is propagating in a forward direction away from the origin with angle θ to the z-axis then,

$$\begin{aligned} \underline{k}^t &= k_t \hat{e}_{\parallel} \\ k_t &= k_0 \sin \theta \\ k_z &= k_0 \cos \theta \end{aligned} \quad (2-34)$$

Note that according to our definitions the incident and transmitted waves point towards the origin, so for these waves $\theta = \pi - \theta_{in} = \pi - \theta_{tx}$ whereas for the reflected wave (which points away) $\theta = \theta_{rx}$.

Now let us write,

$$\underline{H}^t = H_{\parallel} \hat{e}_{\parallel} + H_{\perp} \hat{e}_{\perp} = \begin{pmatrix} H_{\perp} \\ H_{\parallel} \end{pmatrix} \text{ in the TE TM coordinate base.} \quad (2-35)$$

$$\underline{E}^t = E_{\parallel} \hat{e}_{\parallel} + E_{\perp} \hat{e}_{\perp} = \begin{pmatrix} E_{\perp} \\ E_{\parallel} \end{pmatrix} \text{ in the TE TM coordinate base.} \quad (2-36)$$

for arbitrary coefficients H_{\parallel} , H_{\perp} , E_{\parallel} and E_{\perp} . Substituting into (2-33) we obtain the matrix form (in the TE TM coordinate base),

$$\begin{pmatrix} E_{\perp} \\ E_{\parallel} \end{pmatrix} = -\eta_0 \begin{pmatrix} 1/\cos\theta & 0 \\ 0 & \cos\theta \end{pmatrix} \begin{pmatrix} 0 & 1 \\ -1 & 0 \end{pmatrix} \begin{pmatrix} H_{\perp} \\ H_{\parallel} \end{pmatrix} \quad (2-37)$$

We require in a Cartesian coordinate system, such that

$$\underline{H}^t = H_x \hat{x} + H_y \hat{y} \quad (2-38)$$

$$\underline{E}^t = E_x \hat{x} + E_y \hat{y} \quad (2-39)$$

Transforming between coordinate systems, define

$$\mathbf{v} = \mathbf{v}^T = \begin{pmatrix} -\sin\phi & \cos\phi \\ \cos\phi & \sin\phi \end{pmatrix} \quad (2-40)$$

then

$$\begin{pmatrix} E_x \\ E_y \end{pmatrix} = \mathbf{v} \begin{pmatrix} 1/\cos\theta & 0 \\ 0 & \cos\theta \end{pmatrix} \mathbf{J} \cdot \mathbf{v} \cdot \begin{pmatrix} H_x \\ H_y \end{pmatrix} \quad (2-41)$$

since $\mathbf{J} \mathbf{v} = -\mathbf{v} \mathbf{J}$ we may write,

$$\begin{pmatrix} E_x \\ E_y \end{pmatrix} = +\eta_0 \mathbf{W}(\theta, \phi) \mathbf{J} \begin{pmatrix} H_x \\ H_y \end{pmatrix} \quad (2-42)$$

where

$$\mathbf{W}(\theta, \phi) = \mathbf{v}(\phi) \begin{pmatrix} 1/\cos\theta & 0 \\ 0 & \cos\theta \end{pmatrix} \mathbf{v}(\phi) \quad (2-43)$$

Now, for consistency with [1] let us define $\mathbf{W}(\theta, \phi)$ evaluated when $\theta = \theta_{in}$ and $\phi = \phi_{in}$. These, in our notation, are the required values for a *reflected* wave. Thus define $\mathbf{W} \equiv \mathbf{W}(\theta_{in}, \phi_{in})$ in which case,

$$\mathbf{W} = \cos\theta_{in} \begin{pmatrix} \cos^2\phi_{in} & \cos\phi_{in}\sin\phi_{in} \\ \cos\phi_{in}\sin\phi_{in} & \sin^2\phi_{in} \end{pmatrix} + \frac{1}{\cos\theta_{in}} \begin{pmatrix} \sin^2\phi_{in} & -\cos\phi_{in}\sin\phi_{in} \\ -\cos\phi_{in}\sin\phi_{in} & \cos^2\phi_{in} \end{pmatrix} \quad (2-44)$$

and its inverse,

$$\mathbf{W}^{-1} = \frac{1}{\cos\theta_{in}} \begin{pmatrix} \cos^2\phi_{in} & \cos\phi_{in}\sin\phi_{in} \\ \cos\phi_{in}\sin\phi_{in} & \sin^2\phi_{in} \end{pmatrix} + \cos\theta_{in} \begin{pmatrix} \sin^2\phi_{in} & -\cos\phi_{in}\sin\phi_{in} \\ -\cos\phi_{in}\sin\phi_{in} & \cos^2\phi_{in} \end{pmatrix} \quad (2-45)$$

In order to relate the tangential fields at either side of the structure to \mathcal{R} and \mathcal{T} , it is necessary to decompose the free-space fields into incident, reflected and transmitted waves. This is the so-called *wave-splitting* method which is straightforward to do in an isotropic

material. Equations (1-9) decompose the full wave into incident, reflected and transmitted parts. Associated with each we may consider the tangential components. In the left hand half plane there is an incident and reflected wave and in the right hand half plane there is a transmitted and a possible incoming wave (which is assumed not present for a complete free structure). In Cartesian coordinates we write,

$$\underline{E}_{xy}(z) = \begin{pmatrix} E_x(z) \\ E_y(z) \end{pmatrix} = \underline{F}^+(z, \theta)|_{\theta=\pi-\theta_{in}} + \underline{F}^-(z, \theta)|_{\theta=\theta_{in}} \quad (2-46)$$

and

$$\underline{H}_{xy}(z) = \begin{pmatrix} H_x(z) \\ H_y(z) \end{pmatrix} = \underline{G}^+(z, \theta)|_{\theta=\pi-\theta_{in}} + \underline{G}^-(z, \theta)|_{\theta=\theta_{in}} \quad (2-47)$$

where the superscript “+” refers to a wave propagating from the left to the right half plane and the “-” refers to a wave propagating from the right to the left half plane. To simplify notation (and in keeping with [1]) define,

$$\begin{aligned} \underline{F}^+(z) &= \underline{F}^+(z, \theta_{in}) \\ \underline{F}^-(z) &= \underline{F}^-(z, \theta_{in}) \\ \underline{G}^+(z) &= \underline{G}^+(z, \theta_{in}) \\ \underline{G}^-(z) &= \underline{G}^-(z, \theta_{in}) \end{aligned} \quad (2-48)$$

Since $\mathbf{W}(\theta_{in}, \phi_{in}) = -\mathbf{W}(\pi - \theta_{in}, \phi_{in})$ equation (2-42) implies,

$$\eta_0 \mathbf{J} \cdot \underline{G}^\pm(z) = \mp \mathbf{W}^{-1} \underline{F}^\pm(z) \quad (2-49)$$

which is Rikte et al’s result.

We now substitute (2-49) into (2-26) to obtain [1],

$$\begin{pmatrix} \underline{F}^+(z_{N-1}) \\ \underline{F}^-(z_{N-1}) \end{pmatrix} = \begin{pmatrix} \mathbf{T}_{11} & \mathbf{T}_{12} \\ \mathbf{T}_{21} & \mathbf{T}_{22} \end{pmatrix} \cdot \begin{pmatrix} \underline{F}^+(z_1) \\ \underline{F}^-(z_1) \end{pmatrix} \quad (2-50)$$

where

$$\begin{aligned} 2\mathbf{T}_{11} &= \mathbf{P}_{11} - \mathbf{P}_{12} \cdot \mathbf{W}^{-1} - \mathbf{W} \cdot \mathbf{P}_{21} + \mathbf{W} \cdot \mathbf{P}_{22} \cdot \mathbf{W}^{-1} \\ 2\mathbf{T}_{12} &= \mathbf{P}_{11} + \mathbf{P}_{12} \cdot \mathbf{W}^{-1} - \mathbf{W} \cdot \mathbf{P}_{21} - \mathbf{W} \cdot \mathbf{P}_{22} \cdot \mathbf{W}^{-1} \\ 2\mathbf{T}_{21} &= \mathbf{P}_{11} - \mathbf{P}_{12} \cdot \mathbf{W}^{-1} + \mathbf{W} \cdot \mathbf{P}_{21} - \mathbf{W} \cdot \mathbf{P}_{22} \cdot \mathbf{W}^{-1} \\ 2\mathbf{T}_{22} &= \mathbf{P}_{11} + \mathbf{P}_{12} \cdot \mathbf{W}^{-1} + \mathbf{W} \cdot \mathbf{P}_{21} + \mathbf{W} \cdot \mathbf{P}_{22} \cdot \mathbf{W}^{-1} \end{aligned} \quad (2-51)$$

where the 2×2 matrices \mathbf{P}_{ij} are the submatrices of $\underline{\underline{P}}^{(4)}(z_{N-1}, z_1)$,

$$\underline{\underline{P}}^{(4)}(z_{N-1}, z_1) \equiv \begin{pmatrix} \mathbf{P}_{11} & \mathbf{P}_{12} \\ \mathbf{P}_{21} & \mathbf{P}_{22} \end{pmatrix} \quad (2-52)$$

At this point we define the tangential reflection and transmission coefficient matrices, \underline{r} and \underline{t} such that,

$$\begin{aligned}\underline{F}^-(z_1) &= \mathbf{r} \underline{F}^+(z_1) \\ \underline{F}^+(z_{N-1}) &= \mathbf{t} \underline{F}^+(z_1)\end{aligned}\quad (2-53)$$

with components,

$$\mathbf{r} = \begin{pmatrix} r_{xx} & r_{xy} \\ r_{yx} & r_{yy} \end{pmatrix} \quad (2-54)$$

and

$$\mathbf{t} = \begin{pmatrix} t_{xx} & t_{xy} \\ t_{yx} & t_{yy} \end{pmatrix} \quad (2-55)$$

These matrices are given by,

$$\left. \begin{aligned} \mathbf{r} &= -\mathbf{T}_{22}^{-1} \cdot \mathbf{T}_{21} \\ \mathbf{t} &= \mathbf{T}_{11} + \mathbf{T}_{12} \cdot \mathbf{r} \end{aligned} \right\} \text{ for a free structure} \quad (2-56)$$

for a free structure. In the special case where the structure is terminated by a perfect conductor, these matrices are not properly defined. In this case $\underline{E}_{xy}(z_{N-1}) = 0$ and the first row of (2-26) is given by,

$$\underline{0} = (\mathbf{P}_{11} \ \mathbf{P}_{12}) \begin{pmatrix} \mathbf{I} & \mathbf{I} \\ -\mathbf{W}^{-1} & \mathbf{W}^{-1} \end{pmatrix} \begin{pmatrix} \underline{F}^+(z_1) \\ \mathbf{r} \cdot \underline{F}^+(z_1) \end{pmatrix} \quad (2-57)$$

giving,

$$\left. \begin{aligned} \mathbf{r} &= -(\mathbf{P}_{11} + \mathbf{P}_{12} \cdot \mathbf{W}^{-1})^{-1} \cdot (\mathbf{P}_{11} - \mathbf{P}_{12} \cdot \mathbf{W}^{-1}) \\ \mathbf{t} &= 0 \end{aligned} \right\} \text{ for a PEC terminated structure} \quad (2-58)$$

2.3.5 Determination of the reflectance and transmittance matrices

The physical quantities of interest are the reflectance and transmittance matrices, \mathcal{R} and \mathcal{T} , which express the reflection and transmission coefficients in dB and phase for a wave incident on the material. In order to obtain \mathcal{R} and \mathcal{T} we transform back into a TM TE coordinate base. We therefore define ⁶

$$\mathbf{r}' = \begin{pmatrix} r_{\parallel\parallel} & r_{\parallel\perp} \\ r_{\perp\parallel} & r_{\perp\perp} \end{pmatrix} = \mathbf{u} \mathbf{r} \mathbf{u}^T \quad (2-59)$$

and

$$\mathbf{t}' = \begin{pmatrix} t_{\parallel\parallel} & t_{\parallel\perp} \\ t_{\perp\parallel} & t_{\perp\perp} \end{pmatrix} = \mathbf{u} \mathbf{t} \mathbf{u}^T \quad (2-60)$$

⁶The order of entries is merely for historical reasons and matches the order of entries in the computer software.

where

$$\mathbf{u} = \begin{pmatrix} \cos \phi_{in} & \sin \phi_{in} \\ -\sin \phi_{in} & \cos \phi_{in} \end{pmatrix} \quad (2-61)$$

so that we may finally identify (see [2] for details of the derivation of full wave from tangential coefficients),

$$\mathcal{T} = \begin{pmatrix} \mathcal{T}_{\perp\perp} & \mathcal{T}_{\parallel\perp} \\ \mathcal{T}_{\perp\parallel} & \mathcal{T}_{\parallel\parallel} \end{pmatrix} = \begin{pmatrix} t_{\perp\perp} & -t_{\parallel\perp}/\cos\theta_{in} \\ -t_{\perp\parallel}\cos\theta_{in} & t_{\parallel\parallel} \end{pmatrix} \quad (2-62)$$

and

$$\mathcal{R} = \begin{pmatrix} \mathcal{R}_{\perp\perp} & \mathcal{R}_{\parallel\perp} \\ \mathcal{R}_{\perp\parallel} & \mathcal{R}_{\parallel\parallel} \end{pmatrix} = \begin{pmatrix} r_{\perp\perp} & +r_{\parallel\perp}/\cos\theta_{in} \\ -r_{\perp\parallel}\cos\theta_{in} & -r_{\parallel\parallel} \end{pmatrix} \quad (2-63)$$

2.4 The transverse formulation method 2

2.4.1 Introduction - extensions to method 1

We wish to extend the method to permit an impedance surface, of general electric anisotropic form, to lie at the interface of any or all of the layers in the multi-layer structure. This is illustrated in figure 2-2. Note the change in the numbering convention compared with figure 2-1 and the use of $i = 0$ and $i = N + 1$ to refer to the left hand and right hand (free space) semi-infinite materials to the left and right of the structure.

Such an impedance surface is defined as thin, i.e. of essentially zero thickness, anisotropic with two orthogonal principal axes, and realisable. For it to be realisable we preclude the possibility of magnetic currents (lacking the existence of magnetic monopoles) and thus the tangential electric field is assumed to be continuous across the interface.

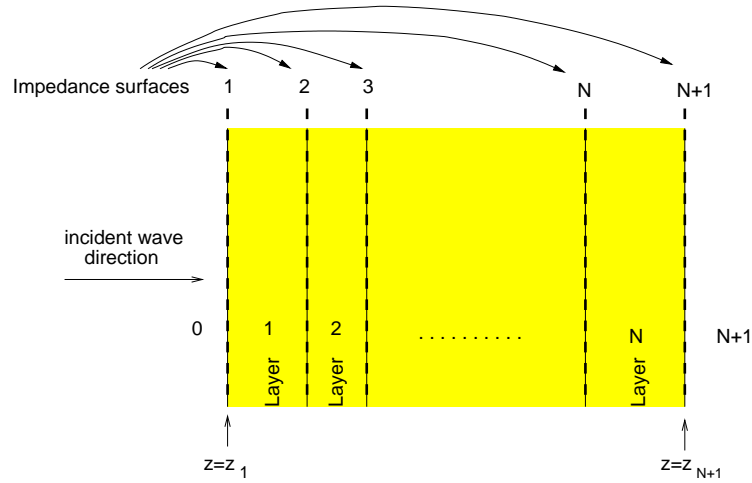


Figure 2-2: A structure consisting of N layers with impedance surfaces between layers.

To describe the electrical behaviour of such an interface, let the field just to the left of the interface be designated by a superfix ‘-’ and just to the right by a superfix ‘+’. The vector field pair,

$$\begin{pmatrix} \underline{E}_{xy}^-(z_i) \\ \eta_0 \underline{J}_2 \cdot \underline{H}_{xy}^-(z_i) \end{pmatrix}$$

designates the tangential electric and rotated magnetic field just to the left of the interface at $z = z_i$ and the vector field pair,

$$\begin{pmatrix} \underline{E}_{xy}^+(z_i) \\ \eta_0 \underline{J}_2 \cdot \underline{H}_{xy}^+(z_i) \end{pmatrix}$$

designates the tangential electric and rotated magnetic field just to the right of the interface at $z = z_i$. The boundary conditions applied to the interface are given by,

$$\underline{E}_{xy}^-(z_i) = \underline{E}_{xy}^+(z_i) \quad (2-64)$$

and

$$\eta_0 \underline{\underline{J}}_2 \cdot (\underline{H}_{xy}^+(z_i) - \underline{H}_{xy}^-(z_i)) = \eta_0 \boldsymbol{\sigma} \cdot \underline{E}_{xy}^-(z_i) \quad (2-65)$$

where $\boldsymbol{\sigma}$ is the 2×2 conductivity tensor, with units in Ohms⁻¹, defined by

$$\boldsymbol{\sigma} = \mathbf{R}^T \boldsymbol{\Sigma} \mathbf{R} \quad (2-66)$$

where $\boldsymbol{\Sigma}$ is the diagonal matrix defining the principal value conductivities,

$$\boldsymbol{\Sigma} = \begin{pmatrix} \sigma^\perp & 0 \\ 0 & \sigma^\parallel \end{pmatrix} \quad (2-67)$$

and \mathbf{R} is the real symmetric rotation matrix (assumed independent of frequency),

$$\mathbf{R} = \begin{pmatrix} \cos \nu & -\sin \nu \\ \sin \nu & \cos \nu \end{pmatrix} \quad (2-68)$$

for real rotation angle ν . σ^\perp and σ^\parallel are generally complex frequency dependent conductivities expressed in Ohms⁻¹. Realisable forms for these may be given using equivalent circuit models, as described in section 2.7. These relations are formally exact, but only if σ^\perp and σ^\parallel are known. However, they can often be estimated using approximate techniques (e.g. using approximate boundary conditions and/or low frequency methods) and used to *model* the behaviour of a real frequency selective surfaces embedded in real materials. The true structures they represent might be formed using periodic patterns of thin regions of conductor (e.g. copper) and/or resistive materials (e.g. carbon or indium tin oxide) with/without lumped passive or (possibly) semiconductor materials.⁷

One example, employed later, of a simple anisotropic surface is a polarising grid with strip width and inter-strip spacings small (but not very small) compared to a wavelength. In this case the angle ν defines the grid angle, $\sigma^\perp = 0$ and $\sigma^\parallel \rightarrow \infty$. A more accurate model requires capacitive and inductive models; $\sigma^\perp \sim j\omega C$ and $\sigma^\parallel \sim 1/(j\omega L)$ where ωC and ωL are small.

Combining (2-64) and (2-65) and using a subscript i to refer to the values for the i_{th} interface we obtain,

$$\begin{pmatrix} \underline{E}_{xy}^+(z_i) \\ \eta_0 \underline{\underline{J}}_2 \cdot \underline{H}_{xy}^+(z_i) \end{pmatrix} = \underline{\underline{S}}_i^{-1} \begin{pmatrix} \underline{E}_{xy}^-(z_i) \\ \eta_0 \underline{\underline{J}}_2 \cdot \underline{H}_{xy}^-(z_i) \end{pmatrix} \quad (2-69)$$

where

$$\underline{\underline{S}}_i = \begin{pmatrix} \mathbf{I} & 0 \\ -\eta_0 \mathbf{R}_i^T \boldsymbol{\Sigma}_i \mathbf{R}_i & \mathbf{I} \end{pmatrix} \quad (2-70)$$

\mathbf{I} is the 2×2 identity matrix. The inverse,

$$\underline{\underline{S}}_i^{-1} = \begin{pmatrix} \mathbf{I} & 0 \\ \eta_0 \mathbf{R}_i^T \boldsymbol{\Sigma}_i \mathbf{R}_i & \mathbf{I} \end{pmatrix} \quad \text{for } i = 1 \text{ to } N + 1 \quad (2-71)$$

⁷The accurate determination of the equivalent conductivities of FSS embedded in a general bianisotropic composite is a task requiring advanced numerical techniques outside of the scope of this formulation. Commercial software packages such as CST [10] or HFSS [11] may be used for this purpose.

It is possible to employ this relation directly within the previously described method-1 concatenation, replacing (2-27) by the concatenation,

$$\begin{aligned} \underline{\underline{P}}^{(4)}(z_{N-1}, z_1) &= \underline{\underline{S}}^{-1}(z_{N-1}) \exp(-jk_0(z_{N-1} - z_{N-2})\underline{\underline{M}}_{N-1}^{(4)}) \\ &\quad \underline{\underline{S}}^{-1}(z_{N-2}) \exp(-jk_0(z_{N-2} - z_{N-3})\underline{\underline{M}}_{N-2}^{(4)}) \\ &\quad \dots \underline{\underline{S}}^{-1}(z_2) \exp(-jk_0(z_2 - z_1)\underline{\underline{M}}_2^{(4)}) \underline{\underline{S}}^{-1}(z_1) \end{aligned} \quad (2-72)$$

This method was adopted within an interim version (version 00.02.00) of the software but can be seriously ill-conditioned when any/all of the $\underline{\underline{S}}$ matrices contain both very small and very large terms. The reason for this is that such structures are opaque to one polarisation and thus fail for the reasons outlined previously. We will not consider this concatenation method any further, except by way of a later example illustrating the problem.

2.4.2 Partial waves revisited

Although, for the reasons outlined previously, we are not able to provide a precise and uniformly valid partial wave analysis for general bianisotropic materials, we are able to provide a similar method based on a singular value decomposition (SVD) of the $\underline{\underline{P}}$ matrices. We will call this a *quasi partial wave* analysis. In what follows we begin with a description of a “proper” eigenmode analysis and describe some of the problems involved. We then proceed with the SVD, showing some relationships and some important differences between the two approaches.

A (full) partial wave analysis decomposes the total tangential electric and magnetic fields on either side of an interface in terms of the tangential components of “forwards” and “backwards” wave components that correspond to the *eigenmodes* within the medium the given side of the interface. These wave components represent a set of linear combinations of the \underline{E}_{xy} and $\eta_0 \underline{J}_2 \underline{H}_{xy}$ vector fields, dependent on the constitutive properties of the layer but independent of the position within the layer. Within the layer, we may write this set of linear combinations by the 4×4 matrix $\underline{\underline{\alpha}}$ such that,

$$\underline{\underline{\alpha}} \begin{pmatrix} \underline{E}_{xy}(z) \\ \eta_0 \underline{J}_2 \underline{H}_{xy}(z) \end{pmatrix} = \begin{pmatrix} l_1(z) & 0 & 0 & 0 \\ 0 & l_2(z) & 0 & 0 \\ 0 & 0 & l_3(z) & 0 \\ 0 & 0 & 0 & l_4(z) \end{pmatrix} \underline{\underline{\alpha}} \begin{pmatrix} \underline{E}_{xy}(z_i) \\ \eta_0 \underline{J}_2 \underline{H}_{xy}(z_i) \end{pmatrix} \text{ for } z_i < z < z_{i+1} \quad (2-73)$$

and formally we may identify,

$$\underline{\underline{P}}^{(4)}(z_{i+1}, z_i) = \underline{\underline{\alpha}}^{-1} \begin{pmatrix} l_1 & 0 & 0 & 0 \\ 0 & l_2 & 0 & 0 \\ 0 & 0 & l_3 & 0 \\ 0 & 0 & 0 & l_4 \end{pmatrix} \underline{\underline{\alpha}} \quad (2-74)$$

Such a diagonalisation is obtained if the rows of $\underline{\underline{\alpha}}$ are the eigenmodes of the medium, expressed in the $(\underline{E}, \eta_0 \underline{J}_2, \underline{H})$ base, and the $l_k(z)$ represent the complex modal propagation factors whose magnitude and phase are generally both functions of z .

Suppose $\underline{\underline{M}}_i$ is that matrix $\underline{\underline{M}}^{(4)}$, independent of z , corresponding to the i_{th} layer. Because $\underline{\underline{P}}^{(4)}(z, z_i)$, for $z_{i+1} < z < z_i$, takes the form (2-25) it follows that provided $-jk_0(z - z_i)\underline{\underline{M}}_i$ can be diagonalised by

$$-jk_0(z - z_i)\underline{\underline{M}}_i = \underline{\underline{\beta}}^{-1} \begin{pmatrix} -jk_0(z - z_i) m_1 & 0 & 0 & 0 \\ 0 & -jk_0(z - z_i) m_2 & 0 & 0 \\ 0 & 0 & -jk_0(z - z_i) m_3 & 0 \\ 0 & 0 & 0 & -jk_0(z - z_i) m_4 \end{pmatrix} \underline{\underline{\beta}}$$

with a matrix $\underline{\underline{\beta}}$ whose inverse $\underline{\underline{\beta}}^{-1}$ exists, then matrix exponential theory implies that,

$$\underline{\underline{\beta}} = \underline{\underline{\alpha}} \quad (2-75)$$

and the complex eigenvalues are related by,

$$l_k = \exp(-jk_0(z - z_i)m_k) \quad \text{for } k = 1, 2, 3, 4 \quad (2-76)$$

and hence the matrix of eigenmodes, $\underline{\underline{\alpha}}$, is independent of z because $\underline{\underline{\beta}}$ is independent of z . Because the matrix $\underline{\underline{M}}_i$ is *not* Hermitian (indeed it is not even a normal matrix) we can say little in general about the nature of the eigenvalues, m_k . However, for lossless isotropic materials m_i are real and hence l_k have unit magnitude. This also appears to be true for several classes of lossless anisotropic materials. Note that if $\underline{\underline{\beta}}^{-1}$ does not exist, and this occurs for rank deficient matrices, then (2-75) does not generally hold true and $\underline{\underline{\alpha}}$ may become dependent on z . Rank deficiency is known to occur for certain angles of incidence in certain special kinds of anisotropic materials.

If one or more of the $l_k(z)$ take the same value then $\underline{\underline{\alpha}}$ is not unique. There are differing physical interpretations depending on the nature of the degeneracy.

For example, in an isotropic medium, there are generally two pairs of distinct eigenvalues since there is no difference in wave propagation when the direction of the electric field is rotated about the direction of propagation. In this case there are only two eigenmodes corresponding to the forwards and backwards travelling waves. Another situation arises when the thickness of the layer approaches zero. In this case $\underline{\underline{P}}^{(4)} \rightarrow \underline{\underline{I}}$, the identity matrix, and it becomes impossible to determine the eigenmodes from the matrix $\underline{\underline{P}}^{(4)}$. A similar situation arises in an isotropic medium at normal incidence when $\epsilon_r = \mu_r$. These examples serve to show problems that may be encountered in trying to uniquely determine the partial wave modes from a knowledge only of $\underline{\underline{P}}^{(4)}(z_i, z_{i+1})$ when a material is almost isotropic or when the material is electrically thin, even when $\underline{\underline{\beta}}^{-1}$ exists.

However, while determining the partial wave modes may be desirable, it is not entirely necessary. The ill-conditioning in determination of the transmission and reflection coefficients arises principally because of the existence of exponentially growing terms in $\underline{\underline{P}}^{(4)}$ that occur when loss is present or when some other “loss of information” occurs when we introduce the sheet interface media described earlier.

When loss is present the $l_k(z)$ contain terms that grow or decay exponentially with z . Since $\underline{\underline{P}}^{(4)}$ defines the fields at $z_{i+1} > z_i$ given the fields at z_i , a forwards propagating wave contains terms which decay exponentially with z and a backwards propagating wave terms which grow exponentially with z . Because there are two forwards and two backward waves there must be a pair of l_i values at least one of whose magnitude becomes exponentially large as the layer thickness and/or the loss factor becomes large. Similarly, the second pair must feature at least one value whose magnitude become exponentially small.

Somehow, we need to regroup the fields at z_i and z_{i+1} so that something similar to a reflected backwards propagating wave at z_i and a transmitted forwards propagating wave at z_{i+1} are determined as a function of the backwards incoming wave at z_i and the forwards incoming wave at z_{i+1} . This interpretation would be precise if we had a true partial wave decomposition. However, all that is required is a similarity such that the “exit” fields contain no exponentially large terms in the dependence on the “entry” fields. One possibility is to use the eigenvalue magnitudes in order to re-group the fields (eigenvectors, when they are unique) as “exit” “entry” pairs.

Motivated by this philosophy, instead of performing the eigenvalue decomposition of $\underline{\underline{P}}^{(4)}$, we perform its singular value decomposition (SVD). This has various advantages. Firstly, the SVD is inherently better conditioned than the eigenvalue decomposition. Secondly, we are only interested in the magnitudes of the eigenvalues. There are important differences, though.

If $\underline{\underline{P}}^{(4)}$ is a normal matrix, the singular values of the SVD and the magnitudes of the eigenvalues take the same values. Also, the singular vectors would be (up to a constant phase factor) the same as the eigenvectors and hence independent of z except possibly in degenerate cases. However, as previously mentioned, $\underline{\underline{P}}^{(4)}$ is *not* a normal matrix. Consequently the singular vectors are dependent on layer thickness and the singular values have magnitudes that vary with z . For example, the singular values do not have unit magnitude for a lossless isotropic material and oscillate with z between defined bounds. Also, they assume four different values at non-normal incidence.

With the SVD we have,

$$\underline{\underline{P}}^{(4)}(z_{i+1}, z_i) = \underline{\underline{V}}_{i+1} \begin{pmatrix} \lambda_1 & 0 & 0 & 0 \\ 0 & \lambda_2 & 0 & 0 \\ 0 & 0 & \lambda_3 & 0 \\ 0 & 0 & 0 & \lambda_4 \end{pmatrix} \underline{\underline{U}}_{i+1}^{-1} \text{ for } i = 1, N \quad (2-77)$$

where $\underline{\underline{V}}$ and $\underline{\underline{U}}$ are unitary matrices (such that the inverses are equal to the complex conjugate transposes, $\underline{\underline{U}}^{-1} = \underline{\underline{U}}^\dagger$ and $\underline{\underline{V}}^{-1} = \underline{\underline{V}}^\dagger$) respectively containing the left and right singular vectors entered as columns and μ_i are the (defined positive real) singular values. The λ_i are ordered such that $\lambda_1 \geq \lambda_2 \geq \lambda_3 \geq \lambda_4$.

The decomposition is well conditioned for *any* matrix P though (as given below) we need specific constructions for $\underline{\underline{V}}$ and $\underline{\underline{U}}$ when there is high level degeneracy for which all singular values are equal. Note that $\underline{\underline{V}}$ and $\underline{\underline{U}}$ are both defined in terms of the electrical properties of layer $i + 1$, as illustrated in figure 2-2.

With this ordering of λ_i we define,

$$\underline{p}_{xy}^-(z_{i+1}) \equiv \begin{pmatrix} \underline{p}_1^-(z_{i+1}) \\ \underline{p}_2^-(z_{i+1}) \end{pmatrix} = \underline{\underline{V}}_{i+1}^{-1} \begin{pmatrix} \underline{E}_{xy}^-(z_{i+1}) \\ \eta_0 \underline{J}_{\underline{2}} \cdot \underline{H}_{xy}^-(z_{i+1}) \end{pmatrix} \quad \text{for } i = 1, N \quad (2-78)$$

where the superfix $-$ designates the field vector just to the left of the interface at the designated value of z and

$$\underline{\underline{V}}_{i+1}^{-1} = \underline{\underline{V}}_{i+1}^\dagger \quad \text{for } i = 1, N \quad (2-79)$$

Similarly,

$$\underline{p}_{xy}^+(z_i) \equiv \begin{pmatrix} \underline{p}_1^+(z_i) \\ \underline{p}_2^+(z_i) \end{pmatrix} = \underline{\underline{U}}_{i+1}^{-1} \begin{pmatrix} \underline{E}_{xy}^+(z_i) \\ \eta_0 \underline{J}_{\underline{2}} \cdot \underline{H}_{xy}^+(z_i) \end{pmatrix} \quad \text{for } i = 1, N \quad (2-80)$$

where the superfix $+$ designates the field vector just to the right of the interface at the designated value of z and

$$\underline{\underline{U}}_{i+1}^{-1} = \underline{\underline{U}}_{i+1}^\dagger \quad \text{for } i = 1, N \quad (2-81)$$

Across a layer, between interfaces, we therefore have,

$$\begin{pmatrix} \underline{p}_1^-(z_{i+1}) \\ \underline{p}_2^-(z_{i+1}) \end{pmatrix} = \begin{pmatrix} \lambda_1 & 0 & 0 & 0 \\ 0 & \lambda_2 & 0 & 0 \\ 0 & 0 & \lambda_3 & 0 \\ 0 & 0 & 0 & \lambda_4 \end{pmatrix} \begin{pmatrix} \underline{p}_1^+(z_i) \\ \underline{p}_2^+(z_i) \end{pmatrix} \quad (2-82)$$

We may therefore *define*, the vectors $\underline{p}_1^-(z_{i+1})$, $\underline{p}_2^-(z_{i+1})$, $\underline{p}_1^+(z_i)$ and $\underline{p}_2^+(z_i)$ as *pseudo-partial waves* with the property that the vector magnitudes,

$$\begin{aligned} |\underline{p}_2^-(z_{i+1})| &< K |\underline{p}_1^-(z_{i+1})| \\ |\underline{p}_2^-(z_{i+1})| &< K |\underline{p}_2^+(z_i)| \\ |\underline{p}_1^+(z_i)| &< K |\underline{p}_1^-(z_{i+1})| \\ |\underline{p}_1^+(z_i)| &< K |\underline{p}_2^+(z_i)| \end{aligned} \quad (2-83)$$

for any physical lossy or lossless structure, where K is some constant independent of the layer thickness $z_{i+1} - z_i$. We may therefore identify;

$\underline{p}_2^-(z_{i+1})$ as taking the role of an outgoing wave travelling left to right (transmitted “T” field),

$\underline{p}_1^-(z_{i+1})$ as taking the role of an incoming travelling wave moving right to left (incident “W” field),

$\underline{p}_2^+(z_i)$ as taking the role of an incoming wave travelling left to right (incident “A” field),

$\underline{p}_1^+(z_i)$ as taking the role of an outgoing wave travelling right to left (reflected “R” field).

These \underline{p} vectors are uniquely defined up to a common phase factor $e^{j\psi}$ provided the singular values are distinct (non-degenerate), but are not unique otherwise. However, since they always satisfy the above bounds this lack of uniqueness is not generally a problem, except for certain special cases where further information is required to construct suitable \underline{U} and \underline{V} matrices, as shown later.

The general rule is now to express outgoing pseudo-partial waves only in terms of incoming ones at each layer of the structure. Re-ordering (2-82) we have,

$$\underline{p}_1^+(z_i) = \begin{pmatrix} 1/\lambda_1 & 0 \\ 0 & 1/\lambda_2 \end{pmatrix} \underline{p}_1^-(z_{i+1}) \quad (2-84)$$

$$\underline{p}_2^-(z_{i+1}) = \begin{pmatrix} \lambda_3 & 0 \\ 0 & \lambda_4 \end{pmatrix} \underline{p}_2^+(z_i) \quad (2-85)$$

which are both well conditioned in the sense that $1/\lambda_1$, $1/\lambda_2$, λ_3 and λ_4 always exist and are well behaved.

2.4.3 Computation of the SVD and degenerate singular values

As given in equation (2-77), the SVD is well conditioned and we employ the LAPACK [12] routine ZGESVD for this task. However, while well conditioned the \underline{U} and \underline{V} matrices are non-unique (not simply up to a phase factor) when there is singular value degeneracy. This is not a problem when we have two pairs of equal singular values since the relative ordering of singular vectors associated with λ_1 and λ_2 or between λ_3 and λ_4 is unimportant for our purposes. However, there is a potential problem when all singular values are equal or sufficiently close that the singular vectors incorrectly mix incoming and outgoing pseudo-partial waves. The problem arises because if the singular vectors are incorrectly identified, the method of calculation of the matrix elements \mathbf{X}_{ij}'' described later in section 2.4.5 may fail. In particular, the matrix $(\boldsymbol{\varsigma}_{22}')^{-1}$ may not exist when $\boldsymbol{\Sigma} = 0$. This is because an inappropriate ordering of the singular vectors may leave sub-blocks of $\underline{V}_{=i}^{-1} \underline{U}_{=i+1}$ containing rows or columns of zeros and hence leave the sub-blocks non-invertible.

To avoid the problem we adopt a special procedure if the ratio,

$$\lambda_4/\lambda_1 > 1.0 - \epsilon \quad (2-86)$$

where ϵ is some small non-zero number (currently we use a value $\epsilon = 10^{-6}$). If (2-86) is true, then we define,

$$\begin{aligned} \underline{U} &= \underline{K} \\ \underline{V} &= (1/\lambda_1) \underline{P} \cdot \underline{K} \end{aligned} \quad (2-87)$$

where $\underline{\underline{K}}$ is chosen as a unitary matrix whose 2×2 block sub-matrices are invertible. A real symmetric matrix satisfying this requirement is the Klein matrix,

$$\underline{\underline{K}} = \frac{1}{2} \begin{pmatrix} 1 & 1 & 1 & 1 \\ 1 & -1 & 1 & -1 \\ 1 & 1 & -1 & -1 \\ 1 & -1 & -1 & 1 \end{pmatrix} \quad (2-88)$$

The special form (2-87) satisfies the SVD when all singular values are equal, in such a manner that all 2×2 sub-blocks of $\underline{\underline{U}}$ and $\underline{\underline{V}}$ are invertible (this is not the default equal singular value definition of $\underline{\underline{U}}$ and $\underline{\underline{V}}$ under the ZGESVD algorithm). It may be adopted as a default condition for any SVD calculated in this report and employed as part of a wrapper for the ZGESVD algorithm.

2.4.4 Special $\underline{\underline{U}}$ and $\underline{\underline{V}}$ for the left and right semi-infinite media

In section 2.4.2 we defined $\underline{\underline{U}}_i$ and $\underline{\underline{V}}_i$ for $i = 1$ to N . However, we also require a partial or pseudo-partial wave description in the semi-infinite left hand and right hand half planes. In particular, $\underline{\underline{V}}_0$ and $\underline{\underline{U}}_{N+1}$ and their inverses must be defined.

We are free to do this in various ways, but it is convenient to define them in terms of the *true* partial waves in free space, since these are known and free of the degeneracy problems associated with generic bianisotropic media as previously discussed. There is no SVD employed and it is important to realise that except at normal incidence both $\underline{\underline{V}}_0$ and $\underline{\underline{U}}_{N+1}$ are non-unitary, in contrast to the pseudo-partial waves defined in the layers. This is why we maintain the distinction of notating the inverses of $\underline{\underline{V}}$ and $\underline{\underline{U}}$ as $\underline{\underline{V}}^{-1}$ and $\underline{\underline{U}}^{-1}$ rather than their complex conjugate transposes when we consider an algorithm valid for all $i = 0$ to $N + 1$.

Using (2-44), (2-45), (2-46), (2-48) and (2-49) we may define

$$\begin{aligned} \underline{\underline{p}}_2^-(z_1) &= \sqrt{2} \underline{\underline{F}}^+(z_1) \\ \underline{\underline{p}}_1^-(z_1) &= \sqrt{2} \underline{\underline{F}}^-(z_1) \\ \underline{\underline{p}}_2^+(z_{N+1}) &= \sqrt{2} \underline{\underline{F}}^+(z_{N+1}) \\ \underline{\underline{p}}_1^+(z_{N+1}) &= \sqrt{2} \underline{\underline{F}}^-(z_{N+1}) \end{aligned} \quad (2-89)$$

in which case,

$$\underline{\underline{V}}_0 = \underline{\underline{U}}_{N+1} = \frac{1}{\sqrt{2}} \begin{pmatrix} \underline{\underline{I}} & \underline{\underline{I}} \\ \underline{\underline{W}}^{-1} & -\underline{\underline{W}}^{-1} \end{pmatrix} \quad (2-90)$$

and

$$\underline{\underline{V}}_0^{-1} = \underline{\underline{U}}_{N+1}^{-1} = \frac{1}{\sqrt{2}} \begin{pmatrix} \underline{\underline{I}} & \underline{\underline{W}} \\ \underline{\underline{I}} & -\underline{\underline{W}} \end{pmatrix} \quad (2-91)$$

with the normalisation constant $\sqrt{2}$ in (2-89) chosen only to ensure that (2-90) and (2-91) are of similar form. Note that $\underline{\underline{U}}_0$ and $\underline{\underline{V}}_{N+1}$ are not employed in the algorithm and need not be defined.

2.4.5 Canonical structures

We now choose to concatenate the layered structure one layer at a time, in a manner similar to that employed in [2] for FSS structures or in appendix D of [1]. One general canonical structure and one special case canonical structure are required and one optional special case. The general structure comprises a single layer terminated on its right hand side by a surface impedance sheet of the kind described in section 2.4.1. The mandatory special structure comprises the first interface of the multi-layer structure fronted by a semi-infinite region of free space. The optional special case is that where the final layer is terminated by a perfect conductor.

General case

Figure 2-3 shows a single layer, layer i for $i = 1, N$ terminated by the surface impedance sheet and the associated \underline{p}_i vectors. We now require to find the 2×2 matrix entries, X''_{11} , X''_{12} , X''_{21} and X''_{22} evaluated on the i_{th} layer (i.e. for $i = 1$ to N but to avoid notation complexity the i dependence of the X'' terms is suppressed) defined by,

$$\begin{pmatrix} \underline{p}_2^+(z_{i+1}) \\ \underline{p}_1^+(z_i) \end{pmatrix} = \begin{pmatrix} X''_{11} & X''_{12} \\ X''_{21} & X''_{22} \end{pmatrix} \begin{pmatrix} \underline{p}_2^+(z_i) \\ \underline{p}_1^+(z_{i+1}) \end{pmatrix} \quad \text{for } i = 1 \text{ to } N \quad (2-92)$$

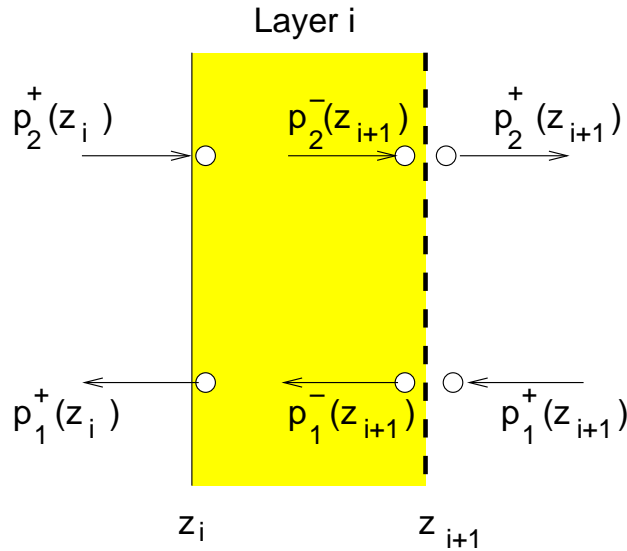


Figure 2-3: The general canonical structure associated with layer i .

Using equations (2-78) and (2-80) together with (2-69) and (2-70) we first relate the \underline{p} vectors either side of the interface at z_{i+1} . This is defined by the matrix $\underline{\varsigma}_i$ composed of 2×2 sub-matrices ς_{11} , ς_{12} , ς_{21} and ς_{22} ,

$$\underline{\varsigma}_i \equiv \begin{pmatrix} \varsigma_{11} & \varsigma_{12} \\ \varsigma_{21} & \varsigma_{22} \end{pmatrix} = \underline{U}_{i+1}^{-1} \underline{S}_{i+1}^{-1} \underline{V}_i \quad \text{for } i = 1 \text{ to } N \quad (2-93)$$

such that

$$\begin{pmatrix} \underline{p}_1^+(z_{i+1}) \\ \underline{p}_2^+(z_{i+1}) \end{pmatrix} = \underline{\Xi}_{i+1} \begin{pmatrix} \underline{p}_1^-(z_{i+1}) \\ \underline{p}_2^-(z_{i+1}) \end{pmatrix} \quad \text{for } i = 1 \text{ to } N \quad (2-94)$$

The inverse matrix is well defined and given by,

$$\underline{\Xi}_i^{-1} \equiv \begin{pmatrix} \underline{\varsigma}'_{11} & \underline{\varsigma}'_{12} \\ \underline{\varsigma}'_{21} & \underline{\varsigma}'_{22} \end{pmatrix} = \underline{V}_i^{-1} \underline{S}_{i+1} \underline{U}_{i+1} \quad \text{for } i = 1 \text{ to } N \quad (2-95)$$

Together with (2-84) and (2-85) this implies,

$$\mathbf{X}''_{11} = (\underline{\varsigma}'_{22})^{-1} \begin{pmatrix} \lambda_3 & 0 \\ 0 & \lambda_4 \end{pmatrix} \quad (2-96)$$

$$\mathbf{X}''_{12} = -(\underline{\varsigma}'_{22})^{-1} \underline{\varsigma}'_{21} \quad (2-97)$$

$$\mathbf{X}''_{21} = \begin{pmatrix} 1/\lambda_1 & 0 \\ 0 & 1/\lambda_2 \end{pmatrix} \underline{\varsigma}'_{12} (\underline{\varsigma}'_{22})^{-1} \begin{pmatrix} \lambda_3 & 0 \\ 0 & \lambda_4 \end{pmatrix} \quad (2-98)$$

$$\mathbf{X}''_{22} = \begin{pmatrix} 1/\lambda_1 & 0 \\ 0 & 1/\lambda_2 \end{pmatrix} (\underline{\varsigma}'_{11} - \underline{\varsigma}'_{12} (\underline{\varsigma}'_{22})^{-1} \underline{\varsigma}'_{21}) \quad (2-99)$$

Provided the pseudo-partial waves are correctly identified, $\underline{p}_2^+(z_{i+1})$ and $\underline{p}_1^+(z_i)$ should have finite magnitudes for any choice of $\underline{p}_2^+(z_i)$ and $\underline{p}_1^+(z_{i+1})$ with finite magnitudes. This implies that \mathbf{X}''_{11} must be bounded and hence $(\underline{\varsigma}'_{22})^{-1}$ must exist provided neither λ_3 nor λ_4 are zero. The existence of $(\underline{\varsigma}'_{22})^{-1}$ is thus assured if there is a unique ordering of the singular value pairs and if neither λ_3 nor λ_4 are zero. The ordering problem for all-equal singular values is addressed and solved in section 2.4.3. So far, we have not come across a problem when λ_3 and/or λ_4 is close to zero (which we expect for very lossy materials) but it should be noted that we have no mathematical proof that $(\underline{\varsigma}'_{22})^{-1}$ always exists under these conditions.

Special case 1 (required)

We now consider the special structure required when the surface is the first interface of the composite. This is illustrated in figure 2-4. and we need to determine the \mathbf{X}''_{ij} matrices defined with

$$\begin{pmatrix} \underline{p}_2^+(z_1) \\ \underline{p}_1^-(z_1) \end{pmatrix} = \begin{pmatrix} \mathbf{X}''_{11} & \mathbf{X}''_{12} \\ \mathbf{X}''_{21} & \mathbf{X}''_{22} \end{pmatrix} \begin{pmatrix} \underline{p}_2^-(z_1) \\ \underline{p}_1^+(z_1) \end{pmatrix} \quad (2-100)$$

We now define,

$$\underline{\Xi}_0 \equiv \begin{pmatrix} \underline{\varsigma}_{11} & \underline{\varsigma}_{12} \\ \underline{\varsigma}_{21} & \underline{\varsigma}_{22} \end{pmatrix} = \underline{U}_1^{-1} \underline{S}_1^{-1} \underline{V}_0 \quad (2-101)$$

such that

$$\begin{pmatrix} \underline{p}_1^+(z_1) \\ \underline{p}_2^+(z_1) \end{pmatrix} = \underline{\Xi}_0 \begin{pmatrix} \underline{p}_1^-(z_1) \\ \underline{p}_2^-(z_1) \end{pmatrix} \quad (2-102)$$

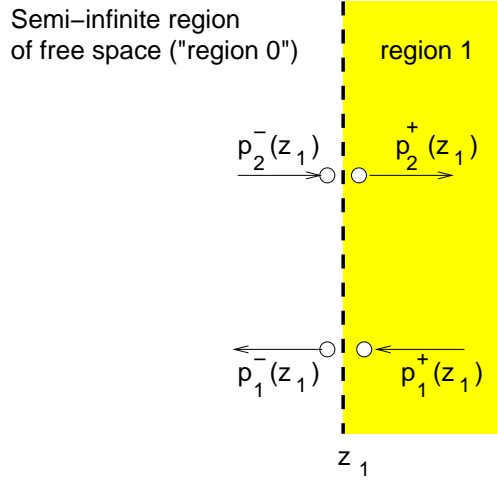


Figure 2-4: The special canonical structure associated with the first interface.

The inverse matrix is well defined and given by,

$$\underline{\zeta}_0^{-1} \equiv \begin{pmatrix} \zeta'_{11} & \zeta'_{12} \\ \zeta'_{21} & \zeta'_{22} \end{pmatrix} = \underline{V}_0^{-1} \underline{S}_1 \underline{U}_1 \quad (2-103)$$

Solution now takes the same form as the general case, with the absence of the diagonal λ matrices,

$$\mathbf{X}''_{11} = (\zeta'_{22})^{-1} \quad (2-104)$$

$$\mathbf{X}''_{12} = -(\zeta'_{22})^{-1} \zeta'_{21} \quad (2-105)$$

$$\mathbf{X}''_{21} = \zeta'_{12} (\zeta'_{22})^{-1} \quad (2-106)$$

$$\mathbf{X}''_{22} = \zeta'_{11} - \zeta'_{12} (\zeta'_{22})^{-1} \zeta'_{21} \quad (2-107)$$

Special case 2 (optional)

We now consider the special structure consisting of a single final layer (layer $i = N$) terminated by a perfect conductor (PEC). This is optional and provides an alternative method of specifying that the final interface is a perfect conductor. The alternative is to specify a general interface with principal conductivities that are both infinite.

In the software, the use of the PEC option in the STRUCTURE definition activates this case, in which case any subsequent definition of an impedance surface at interface $N + 1$ is ignored.

The structure is illustrated in figure 2-5, where we illustrate the case at an arbitrary value of i . and we need to determine the \mathbf{X}''_{ij} matrices defined with

$$\begin{pmatrix} \underline{p}_2^+(z_{i+1}) \\ \underline{p}_1^+(z_i) \end{pmatrix} = \begin{pmatrix} \mathbf{X}''_{11} & \mathbf{X}''_{12} \\ \mathbf{X}''_{21} & \mathbf{X}''_{22} \end{pmatrix} \begin{pmatrix} \underline{p}_2^+(z_i) \\ \underline{p}_1^+(z_{i+1}) \end{pmatrix} \quad (2-108)$$

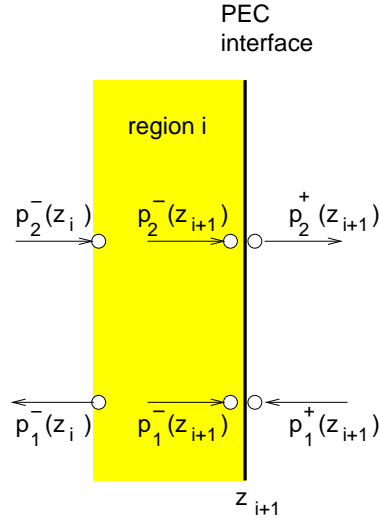


Figure 2-5: The special canonical structure referring to layer terminated by a perfect conductor.

where $\underline{p}_2^+(z_{i+1}) = 0$ and $\underline{p}_1^+(z_i)$ is independent of $\underline{p}_1^+(z_{i+1})$. At the perfect conducting interface, $z = z_{i+1}$, the total tangential electric field is zero, i.e.

$$\begin{aligned}\underline{E}_{xy}^+(z_{i+1}) &= 0 \\ \underline{E}_{xy}^-(z_{i+1}) &= 0\end{aligned}\quad (2-109)$$

These respectively imply that,

$$\underline{\underline{U}}_{i+1} \underline{p}_{xy}^+(z_{i+1}) = \begin{pmatrix} 0 \\ \eta_0 \underline{\underline{J}}_2 \cdot \underline{H}_{xy}^+(z_{i+1}) \end{pmatrix} \quad (2-110)$$

$$\underline{\underline{V}}_i \underline{p}_{xy}^-(z_{i+1}) = \begin{pmatrix} 0 \\ \eta_0 \underline{\underline{J}}_2 \cdot \underline{H}_{xy}^-(z_{i+1}) \end{pmatrix} \quad (2-111)$$

Let us write,

$$\underline{\underline{U}}_{i+1} \equiv \begin{pmatrix} \underline{U}_{11} & \underline{U}_{12} \\ \underline{U}_{21} & \underline{U}_{22} \end{pmatrix} \quad (2-112)$$

$$\underline{\underline{V}}_i \equiv \begin{pmatrix} \underline{V}_{11} & \underline{V}_{12} \\ \underline{V}_{21} & \underline{V}_{22} \end{pmatrix} \quad (2-113)$$

so we have,

$$\begin{aligned}\underline{U}_{11} \underline{p}_1^+(z_{i+1}) + \underline{U}_{12} \underline{p}_2^+(z_{i+1}) &= 0 \\ \underline{V}_{11} \underline{p}_1^-(z_{i+1}) + \underline{V}_{12} \underline{p}_2^-(z_{i+1}) &= 0\end{aligned}\quad (2-114)$$

hence

$$\underline{p}_2^+(z_{i+1}) = -\underline{U}_{12}^{-1} \underline{U}_{11} \underline{p}_1^+(z_{i+1}) \quad (2-115)$$

and

$$\underline{p}_1^+(z_i) = - \begin{pmatrix} 1/\lambda_1 & 0 \\ 0 & 1/\lambda_2 \end{pmatrix} \mathbf{V}_{11}^{-1} \mathbf{V}_{12} \begin{pmatrix} \lambda_3 & 0 \\ 0 & \lambda_4 \end{pmatrix} \underline{p}_2^+(z_i) \quad (2-116)$$

where the λ_k are those referring to the i_{th} layer. Consequently,

$$\mathbf{X}_{11}'' = 0 \quad (2-117)$$

$$\mathbf{X}_{12}'' = -\mathbf{U}_{12}^{-1} \mathbf{U}_{11} \quad (2-118)$$

$$\mathbf{X}_{21}'' = - \begin{pmatrix} 1/\lambda_1 & 0 \\ 0 & 1/\lambda_2 \end{pmatrix} \mathbf{V}_{11}^{-1} \mathbf{V}_{12} \begin{pmatrix} \lambda_3 & 0 \\ 0 & \lambda_4 \end{pmatrix} \quad (2-119)$$

and

$$\mathbf{X}_{22}'' = 0 \quad (2-120)$$

We might implement this special case anywhere within the composite, but it is required only when $i = N$. Since the \underline{p} vectors represent pseudo-partial waves, all the \mathbf{X}_{kl}'' entries must exist. Thus provided \mathbf{U}_{11} and \mathbf{V}_{12} contain no zero eigenvalues (and hence are invertible) then the inverses \mathbf{U}_{12}^{-1} and \mathbf{V}_{11}^{-1} also exist. There is no problem showing existence for the \mathbf{U} matrices when $i = N$, since these refer to the free-space values (2-90). For the \mathbf{V} matrix or for $i \neq N$ we rely on the fact that both \mathbf{U}_{kl} and \mathbf{V}_{kl} are unique, up to a constant phase factor provided there is no singular value degeneracy (discussed previously). We therefore expect existence of the inverses, since if they did not then the layer problem would be inherently badly conditioned, which makes no physical sense. As with the general canonical structure we do not, however, have a mathematical proof of this.

2.4.6 Concatenation with the canonical structures

In order to consider the effect of all layers in the composite we now proceed with a concatenation where we build up the composite a layer at a time starting with the special case canonical structure defined above. We then use the general case canonical structure to represent the effect of each successive layer until we have completed the composite.

Suppose we know the pseudo-partial R and T waves, $\underline{p}_1^-(z_1)$ and $\underline{p}_2^+(z_i)$ given the pseudo-partial incident A and W waves, $\underline{p}_1^+(z_i)$ and $\underline{p}_2^-(z_1)$ for that part of the composite composed of the left hand semi-infinite medium and layers 1 to $i - 1$ (with interfaces 1 to i) and we wish to add the canonical structure comprising layer i with interface $i + 1$, for $i = 1$ to N . This is illustrated in figure 2-6.

Let the connection in the partial composite (layers 1 to $i - 1$ plus the first interface) be defined by the matrix $\underline{\underline{X}}'_i$ with sub-matrices \mathbf{X}'_{kl} ,

$$\begin{pmatrix} \underline{p}_2^+(z_i) \\ \underline{p}_1^-(z_1) \end{pmatrix} = \begin{pmatrix} \mathbf{X}'_{11} & \mathbf{X}'_{12} \\ \mathbf{X}'_{21} & \mathbf{X}'_{22} \end{pmatrix}_i \begin{pmatrix} \underline{p}_2^-(z_1) \\ \underline{p}_1^+(z_i) \end{pmatrix} \quad \text{for } i = 1 \text{ to } N \quad (2-121)$$

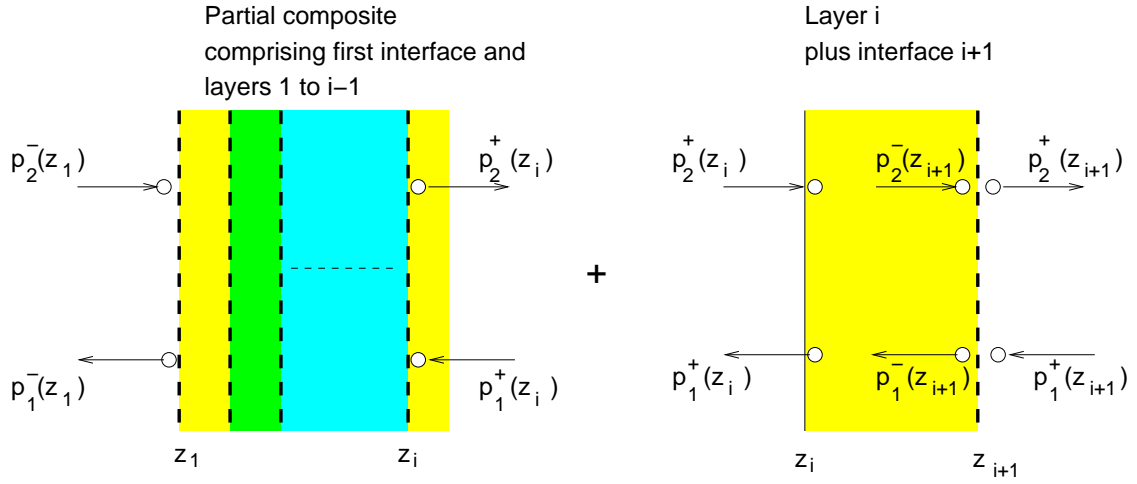


Figure 2-6: Concatenation of partial structure with the next layer.

If $i = N$ then this refers to the complete composite and we need consider no further concatenation. For $i < N$ we suppose that for the layer-plus-interface, for $i \geq 1$, we employ (2-96) to (2-99). The \underline{p} pseudo-partial waves at the centre of the structure must be well defined in terms of the pseudo-partial waves entering the structure at the left of the partial composite and at the right of the i_{th} layer. We find that,

$$\underline{p}_2^+(z_i) = (\mathbf{I} - \mathbf{X}'_{12}\mathbf{X}''_{21})^{-1}\mathbf{X}'_{11}\underline{p}_2^-(z_1) + (\mathbf{I} - \mathbf{X}'_{12}\mathbf{X}''_{21})^{-1}\mathbf{X}'_{12}\mathbf{X}''_{22}\underline{p}_1^+(z_{i+1}) \quad (2-122)$$

$$\underline{p}_1^+(z_i) = \mathbf{X}''_{21}(\mathbf{I} - \mathbf{X}'_{12}\mathbf{X}''_{21})^{-1}\mathbf{X}'_{11}\underline{p}_2^-(z_1) + \left(\mathbf{X}''_{21}(\mathbf{I} - \mathbf{X}'_{12}\mathbf{X}''_{21})^{-1}\mathbf{X}'_{12} + \mathbf{I}\right)\mathbf{X}''_{22}\underline{p}_1^+(z_{i+1})$$

Substituting these expressions into the right hand sides of (2-121) and (2-92) we obtain the new matrix terms for the concatenated structure, defined by the matrix $\underline{\underline{Y}}$, with 2×2 block matrices \mathbf{Y}_{kl} where,

$$\begin{pmatrix} \underline{p}_2^+(z_{i+1}) \\ \underline{p}_1^-(z_1) \end{pmatrix} = \begin{pmatrix} \mathbf{Y}_{11} & \mathbf{Y}_{12} \\ \mathbf{Y}_{21} & \mathbf{Y}_{22} \end{pmatrix} \begin{pmatrix} \underline{p}_2^-(z_1) \\ \underline{p}_1^+(z_{i+1}) \end{pmatrix} \quad (2-123)$$

we obtain,

$$\mathbf{Y}_{11} = \mathbf{L}_1\mathbf{X}'_{11} \quad (2-124)$$

$$\mathbf{Y}_{12} = \mathbf{L}_1\mathbf{X}'_{12}\mathbf{X}''_{22} + \mathbf{X}''_{12} \quad (2-125)$$

$$\mathbf{Y}_{21} = \mathbf{X}'_{21} + \mathbf{X}'_{22}\mathbf{L}_2\mathbf{X}'_{11} \quad (2-126)$$

$$\mathbf{Y}_{22} = \mathbf{X}'_{22}(\mathbf{L}_2\mathbf{X}'_{12} + \mathbf{I})\mathbf{X}''_{22} \quad (2-127)$$

where

$$\mathbf{L}_1 = \mathbf{X}''_{11}(\mathbf{I} - \mathbf{X}'_{12}\mathbf{X}''_{21})^{-1} \quad (2-128)$$

$$\mathbf{L}_2 = \mathbf{X}''_{21}(\mathbf{I} - \mathbf{X}'_{12}\mathbf{X}''_{21})^{-1} \quad (2-129)$$

Because we are employing pseudo-partial waves, the fields at the centre of the structure are guaranteed to exist given the waves entering the structure from the left and right and hence the matrix inverse appearing in the definition for \mathbf{L}_1 and \mathbf{L}_2 must exist.

The algorithm for determining $\underline{\underline{Y}}$ for the entire structure, for which $i = N$, proceeds as:

Step 1. Let $\underline{\underline{X'}} \leftarrow \underline{\underline{X''}}$ for the special case first interface ($i = 0$).

Step 2. Determine $\underline{\underline{Y}}$ for $i = 1$ (layer 1).

Step 3. Let $\underline{\underline{X'}} \leftarrow \underline{\underline{Y}}$.

Step 4. Determine $\underline{\underline{Y}}$ for next value of i and continue loop until $i = N$, in which case $\underline{\underline{X'}}$ is evaluated with $i = N$; $\underline{\underline{X'}} = \underline{\underline{X'_N}}$.

2.4.7 Determination of the tangential transmission and reflection matrices \mathbf{t} and \mathbf{r}

Determination of the \mathbf{t} and \mathbf{r} matrices is trivial in this formulation. In this case we simply have,

$$\begin{aligned} \mathbf{t} &= \mathbf{X}'_{11} \quad \text{when } i = N \\ \mathbf{r} &= \mathbf{X}'_{21} \end{aligned} \quad (2-130)$$

Given \mathbf{t} and \mathbf{r} calculation of the \mathcal{R} and \mathcal{T} matrices follows exactly as before, as given in section 2.3.5.

2.5 Energy measures and subsidiary quantities

Conservation of energy implies that for a passive realisable material, the total fraction of absorbed incident power (converted to heat) is given by,

$$\mathcal{P}_{TE} = |\mathcal{T}_{\perp\perp}|^2 + |\mathcal{T}_{\parallel\perp}|^2 + |\mathcal{R}_{\perp\perp}|^2 + |\mathcal{R}_{\parallel\perp}|^2 \leq 1 \quad (2-131)$$

for an incident TE wave and,

$$\mathcal{P}_{TM} = |\mathcal{T}_{\perp\parallel}|^2 + |\mathcal{T}_{\parallel\parallel}|^2 + |\mathcal{R}_{\perp\parallel}|^2 + |\mathcal{R}_{\parallel\parallel}|^2 \leq 1 \quad (2-132)$$

for an incident TM wave. If the material is lossless then there is equality in both cases. Both \mathcal{P}_{TE} and \mathcal{P}_{TM} are software outputs and provide a useful diagnostic for program functionality. They are also useful for high power applications where (in conjunction with other factors) they may be used to estimate temperature rise due to heating. In general the \mathcal{T} and \mathcal{R} coefficients are complex numbers and express both the phase and amplitude referenced to the first interface ($z = z_1$). The software expresses these quantities with square magnitudes in dB and phase in degrees,

$$\begin{aligned} \mathcal{T}_{**dB} &= 10 \log_{10} |\mathcal{T}_{**}|^2 \\ \mathcal{R}_{**dB} &= 10 \log_{10} |\mathcal{R}_{**}|^2 \end{aligned} \quad (2-133)$$

and

$$\begin{aligned} \mathcal{T}_{**phase} &= (180/\pi) \arctan_2(\Im(\mathcal{T}_{**}), \Re(\mathcal{T}_{**})) \\ \mathcal{R}_{**phase} &= (180/\pi) \arctan_2(\Im(\mathcal{R}_{**}), \Re(\mathcal{R}_{**})) \end{aligned} \quad (2-134)$$

where the $**$ subscript refers to any entry \parallel or \perp and the \arctan_2 function is the angle-unambiguous arc tangent defined by $\arctan_2(y, x) = \arg(x + jy)$ for real x and y .

Since $\underline{\mathcal{T}}$ and $\underline{\mathcal{R}}$ transform a linearly polarised wave of either polarisation state into one of arbitrary polarisation, we may also define the *axial ratio* and *tilt angle* of a transmitted and reflected wave for such an assumed linearly polarised wave. We write,

$$V_1 \equiv |V_1|e^{j\phi_1} = \begin{cases} \mathcal{T}_{\perp\perp} & \hat{\phi}\text{-directed, TE incident wave} \\ \mathcal{T}_{\perp\parallel} & \hat{\theta}\text{-directed, TM incident wave} \end{cases} \quad (2-135)$$

$$V_2 \equiv |V_2|e^{j\phi_2} = \begin{cases} \mathcal{T}_{\parallel\perp} & \hat{\phi}\text{-directed, TE incident wave} \\ \mathcal{T}_{\parallel\parallel} & \hat{\theta}\text{-directed, TM incident wave} \end{cases} \quad (2-136)$$

and similarly for the reflection coefficients with \mathcal{T}_{**} replaced by \mathcal{R}_{**} . Using definitions from [5], let

$$\rho = \frac{V_2}{V_1} \quad (2-137)$$

$$\delta = \phi_2 - \phi_1 \quad (2-138)$$

then the tilt angle is define by,

$$\tau = \frac{1}{2} \arctan_2(2|V_1||V_2| \cos \delta, |V_1|^2 - |V_2|^2) \quad (2-139)$$

and the axial ratio χ given by

$$\chi^2 = \frac{-\gamma + \sqrt{\gamma^2 - 4}}{2} \quad (2-140)$$

where

$$\gamma = -\frac{(|V_1|/|V_2|)^2 + 2 \cos^2 \delta + (|V_2|/|V_1|)^2}{\sin^2 \delta} \quad (2-141)$$

Again, χ is expressed in dB by,

$$\chi_{dB} = 10 \log_{10} \chi^2 \quad (2-142)$$

since $\chi^2 \geq 1$ is real and positive.

2.6 Special types of materials

2.6.1 Isotropic tensors

An isotropic material is defined by one for which,

$$\underline{\underline{\zeta}} = \underline{\underline{\xi}} = 0 \quad (2-143)$$

$$\underline{\underline{\epsilon}} = \epsilon_r \underline{\underline{I}}_3 \quad (2-144)$$

and

$$\underline{\underline{\mu}} = \mu_r \underline{\underline{I}}_3 \quad (2-145)$$

No special data entry is given for such materials, but may be defined using any of the more general input options defined below. For a realisable passive material ϵ_r and μ_r are complex numbers with zero or negative imaginary parts.

2.6.2 Uniaxial tensors

Usually employed to describe the relative permittivity tensor, but also useful to describe the relative permeability tensor. A uniaxial tensor is associated with a tetragonal or hexagonal crystal form. Isotropic tensors are a special case of the uniaxial. The program is structured in such a way that any constitutive tensor of any material may take this form. There is no requirement that tensors share a common set of principal axes. If a tensor $\underline{\underline{\epsilon}}$, $\underline{\underline{\mu}}$, $\underline{\underline{\zeta}}$ or $\underline{\underline{\xi}}$ is expressed by a generic tensor $\underline{\underline{A}}$, then the special uniaxial form is given by

$$\underline{\underline{A}} = a_1(\underline{\underline{I}}_3 - \underline{\underline{\hat{u}}} \underline{\underline{\hat{u}}}) + a_2 \underline{\underline{\hat{u}}} \underline{\underline{\hat{u}}} \quad (2-146)$$

where $\underline{\underline{\hat{u}}}$ is a real unit vector of arbitrary direction and a_1 and a_2 are arbitrary complex numbers. When referring to the relative permittivity or relative permeability, a_1 and a_2 must have zero or negative imaginary part for a realisable material.

In the software, $\underline{\underline{\hat{u}}}$ is defined by un-normalised component inputs (u_1, u_2, u_3) such that

$$\underline{\underline{\hat{u}}} = (u_1, u_2, u_3) / \sqrt{u_1^2 + u_2^2 + u_3^2} \quad (2-147)$$

A general uniaxial tensor is thus specified by two complex and two real independent numbers (6 degrees of freedom). The program assumes a specification of this tensor which is independent of frequency over the designated range of frequencies using the keyword *CONSTANT_UNIAX* (see later for software use).

2.6.3 Orthotropic tensors

An orthotropic tensor is defined as one with three mutually orthogonal real-valued eigenvectors whose directions are fixed in space. Such are associated with an orthotropic material or orthorhombic crystal form where the principal axes of the tensor coincide with the principal axes of the crystal. The orthorhombic structure is described by three perpendicular dyads and is of practical use since artificial structures are relatively easy to make on such a lattice. The tetragonal and cubic crystal forms are special cases of the orthorhombic and the uniaxial and isotropic tensors are special cases of the orthotropic tensor.

As above, usually employed to describe the relative permittivity tensor or relative permeability tensor, the program is structured in such a way that any constitutive tensor of any material may take this form. If a tensor $\underline{\underline{\epsilon}}$, $\underline{\underline{\mu}}$, $\underline{\underline{\zeta}}$ or $\underline{\underline{\xi}}$ is expressed by a generic tensor $\underline{\underline{A}}$, then the special orthotropic form is given by

$$\underline{\underline{A}} = \underline{\underline{U}} \begin{pmatrix} \lambda_1 & 0 & 0 \\ 0 & \lambda_2 & 0 \\ 0 & 0 & \lambda_3 \end{pmatrix} \underline{\underline{U}}^T \quad (2-148)$$

where λ_1 , λ_2 and λ_3 are complex numbers and $\underline{\underline{U}}$ is a real-valued unitary (rotation) matrix of the form,

$$\underline{\underline{U}} = \begin{pmatrix} \cos \gamma & \sin \gamma & 0 \\ -\sin \gamma & \cos \gamma & 0 \\ 0 & 0 & 1 \end{pmatrix} \begin{pmatrix} 1 & 0 & 0 \\ 0 & \cos \beta & \sin \beta \\ 0 & -\sin \beta & \cos \beta \end{pmatrix} \begin{pmatrix} \cos \alpha & \sin \alpha & 0 \\ -\sin \alpha & \cos \alpha & 0 \\ 0 & 0 & 1 \end{pmatrix} \quad (2-149)$$

where α , β and γ are the (real valued) Euler angles. A general orthotropic tensor is thus specified by three complex and three real independent numbers (9 degrees of freedom). When referring to the permittivity or permeability tensors, λ_1 , λ_2 and λ_3 should have zero or negative imaginary parts for passive realisable materials.

The program allows two options for these tensors. Either a specification of this tensor which is independent of frequency over the designated range of frequencies using the keyword *CONSTANT_ORTHOROT* or where the λ_i values are frequency dependent and specified by a user-supplied data file of tabulated data from which the program interpolates. In this option it is assumed that the Euler angles remain independent of frequency.⁸ The keyword used is *TAB_ORTHOROT*.

Under *TAB_ORTHOROT* the real and the imaginary parts of λ_i are interpolated independently under cubic spline interpolation, using the **spline** and **splint** subroutines defined in section 3.3 of [6]. A minimum of three data points are required with an interpolation range that covers the requested frequency range. Natural splines are assumed with zero second derivative on the boundaries of the data set.

⁸General realisable dispersion relations for tensors are not known to us, so this option must be used with care. We have no knowledge of rules concerning realisable frequency dependent changes in the Euler angles associated with more general tensors, e.g. associated with triclinic crystal forms.

2.6.4 general tensors

Most generally, tensors may be entered in Cartesian x-y-z form where $\underline{\underline{\epsilon}}$, $\underline{\underline{\mu}}$, $\underline{\underline{\xi}}$ or $\underline{\underline{\zeta}}$ take the form,

$$\underline{\underline{A}} = \begin{pmatrix} A_{xx} & A_{xy} & A_{xz} \\ A_{yx} & A_{yy} & A_{yz} \\ A_{zx} & A_{zy} & A_{zz} \end{pmatrix} \quad (2-150)$$

It is assumed that A_{**} are defined independent of frequency but may be arbitrary complex numbers. General conditions for realisability of materials are not known, especially when non-zero $\underline{\underline{\xi}}$ and $\underline{\underline{\zeta}}$ are present. Note that it is not necessary for a material to be reciprocal. The keyword employed for such tensors is *CONSTANT_OVERGEN*.

Some general conditions for tensors are known to us, some of which are listed below and may be useful in investigations of physically realisable materials.

Concerning the relative permittivity and permeability tensors

For general lossless anisotropic (e.g. triclinic) structures, in the absence of “magnetic structures” or strong external magnetic fields $\underline{\underline{\epsilon}}$ and $\underline{\underline{\mu}}$ are real symmetric. This implies that the principal directions of the tensors are orthogonal and real; they correspond with orthogonal directions in real space. Note, however, that for triclinic magnetic crystals the principal directions of $\underline{\underline{\epsilon}}$ and $\underline{\underline{\mu}}$ may vary with frequency and will not in general coincide. A proof of this is given in [9] (section 96) combined with [8] (section 125), though it hinges on some very abstract physics depending on time-reversibility which is violated in the presence of large (i.e. a lot larger than the wave field perturbations) magnetic fields, and in the presence of “magnetic structures” or for certain classes of non-linear effects. Unfortunately, what counts as a suitably violating “magnetic structure” is not defined.

In the presence of strong magnetic fields (and presumably other kinds of time-symmetry breaking effects) a lossless material has tensors which are complex Hermitian rather than real symmetric. In this case, the tensor directions are orthogonal but complex and hence do not coincide with directions in real space.

For lossy materials in the absence of time-reversal-breaking effects, $\underline{\underline{\epsilon}}$ and $\underline{\underline{\mu}}$ are complex symmetric (not Hermitian). Both the real and imaginary parts of the tensors are symmetric with real orthogonal principal directions that do not generally coincide.

For lossy materials in the presence of time-reversal-breaking effects, the tensors can be neither complex symmetric nor complex Hermitian. For a passive material the principal values (eigenvalues) must be complex with zero or negative imaginary part. What constraints this places on the matrix terms or on the principal directions is not known to me.

2.7 Surface impedance models

Any models for determining the principal surface admittances σ^\perp and σ^\parallel associated with a surface impedance interface should be physically realisable and obey causality. A convenient way to guarantee this is to model frequency dependence using equivalent circuits. Any number are possible, but currently (as of version 00.03.00 of the software) we have four forms, which are useful for the modelling of simple resonant and non-resonant structures. In what follows, we define

$$Z = \frac{1}{\sigma^\perp} \quad \text{or} \quad Z = \frac{1}{\sigma^\parallel} \quad (2-151)$$

The equivalent circuits are shown in figure 2-7 with Z given as follows:

Model 1

$$Z = R_1 + j\omega L_1 \quad (2-152)$$

Model 2

$$\frac{1}{Z} = \frac{1}{R_1} + j\omega C_1 \quad (2-153)$$

Model 3

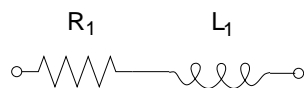
$$Z = R_1 + \frac{1}{j\omega C_1} + j\omega L_1 \quad (2-154)$$

Model 4

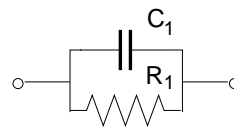
$$\frac{1}{Z} = \frac{1}{R_1} + j\omega C_1 + \frac{1}{j\omega L_1} \quad (2-155)$$

In all cases we must limit the allowed conductivity to some finite value. Too large a value will result in numerical ill-conditioning in the determination of the \mathbf{X}_{kl}'' terms of the canonical layer structures. We limit values so that the minimum value of Z is $\delta = 0.001$ Ohms; i.e.

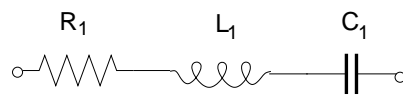
$$\text{if } |Z| < \delta \text{ then define } Z = \delta \quad (2-156)$$



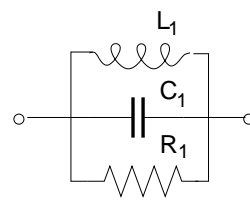
Model 1



Model 2



Model 3



Model 4

Figure 2-7: Equivalent circuit models for the principal surface admittances

3 Software user guide

3.1 Introduction

The software is written in extended Fortran 77, which may be compiled under the Linux operating system using the *gnu g77* or *gfortran* Fortran compiler. At the time of writing, the software version is at version 00.03.002.

It is operated by the name of the executable (*anlay*) followed by the name of the input file:

anlay <input file name>

The input file is a standard ASCII file using key words which are case insensitive. Each line contains one or more key words and numerical parameters. Lines can generally be entered in any order with the main purpose being defined by the first (primary) key word of each line. If a primary key word is not recognised it will be ignored. A list of primary key words are (in no particular order):

FILENAME	Used to designate output file names generated by the software.
STRUCTURE	Top level description of the structure in terms of materials, specified by the MATERIAL type.
ANGLES	Used to define the range of angles of incidence required.
FREQS	Used to define the range of frequencies required.
MATERIAL	Referenced by the STRUCTURE key word. Designates a material by its thickness and TENSOR names used to represent $\underline{\epsilon}$, $\underline{\mu}$, $\underline{\xi}$ and $\underline{\zeta}$.
TENSOR	Referenced by the MATERIAL key word. Defines a tensor by tensor case name and material parameters.
SURFACE	Optional word which, if present, defines a surface impedance sheet associated with the i_{th} interface specified by a rotation angle ν and two principal admittance pointers.
SIGMATYPE	Referenced by the SURFACE key word. Defines the principal admittance specified by a model number and a list of equivalent circuit parameters.

3.2 Key word descriptions

3.2.1 General comments

All key words and numbers are separated by either spaces or commas. Either may be used. Each primary key word is associated to a single line.

3.2.2 FILENAME

Syntax is:

FILENAME <filename1> <filename2>

<filename1> and <filename2> are character strings. They are the names of output files. <filename1> displays data in the same manner as the log file. <filename2> outputs data in column format (see example of output files).

There can be one and only one FILENAME specifier in an input file.

3.2.3 STRUCTURE

Syntax is:

STRUCTURE <n> <type> < $i_1 i_2 \dots i_n$ >

<n> is an integer defining the number of layers.

<type> is a character string which must be either **FREE** or **PEC**. If the former, the structure is assumed to lie in free space with air (vacuum) as the left and right half spaces. If the latter, it is assumed that the structure is terminated by a perfect conductor on its right hand side.

The integers i_1 to i_n are positive integers. There must be n of them but they need not be unique. Each number refers to a MATERIAL type defined below. The materials to which they refer must be defined, but materials can be defined which are not used in the structure. The numbers reference in sequence, starting from the left-most material on which the incident wave impinges to the right-most material, the materials employed in the multi layer structure.

There can be one and only one STRUCTURE specifier in an input file.

3.2.4 ANGLES

Syntax is:

ANGLES < θ_s > < θ_δ > < n_θ > < ϕ_s > < ϕ_δ > < n_ϕ >

This specifies the requested range of incident angles defined by,

$$\begin{aligned}\theta_{in} &= \theta_s + (i - 1)\theta_\delta \\ \phi_{in} &= \phi_s + (j - 1)\phi_\delta\end{aligned}$$

for all integers $1 \leq i \leq n_\theta$ and $1 \leq j \leq n_\phi$.

θ_s , θ_δ , ϕ_s and ϕ_δ are real numbers specified in degrees. n_θ and n_ϕ are positive integers greater than or equal to one.

There can be one and only one ANGLES specifier in an input file.

3.2.5 FREQS

Syntax is:

FREQS < f_s > < f_δ > < n_f >

This specifies the requested range of frequencies defined by,

$$f = f_s + (k - 1) * f_\delta$$

for all integers $1 \leq k \leq n_f$.

f_s and f_δ are real numbers specified in MHz. n_f is a positive integer greater than or equal to one.

There can be one and only one FREQS specifier in an input file.

3.2.6 MATERIAL

Syntax is:

MATERIAL <itype> <thickness> <epsilon_name> <mu_name> <xi_name> <zeta_name>

<itype> is a positive integer specifier used in the STRUCTURE definition. <itype> must be unique to each MATERIAL.

<thickness> is a real number specifying the thickness of the layer of material in meters.

<epsilon_name> is a character string defining the name of the relative permittivity tensor, $\underline{\underline{\epsilon}}$, defined by a TENSOR key word.

<mu_name> is a character string defining the name of the relative permeability tensor, $\underline{\underline{\mu}}$, defined by a TENSOR key word.

<xi_name> is a character string defining the name of the chirality tensor, $\underline{\underline{\xi}}$, defined by a TENSOR key word.

<zeta_name> is a character string defining the name of the chirality tensor, $\underline{\underline{\zeta}}$, defined by a TENSOR key word.

There can be any number of MATERIAL specifiers, more than are necessary to define the material. However there must be sufficient MATERIAL specifiers to do so. If a STRUCTURE definition refers to a MATERIAL specifier <itype> that does not exist, the program will close with an appropriate error message.

3.2.7 TENSOR

Syntax is:

TENSOR <material_name> <tensor_type> {list of parameters}

<material_name> is the name referenced by the MATERIAL definition and must match one of the material names so defined. Each TENSOR definition must have a unique <material_name> or else the program will terminate with a suitable warning.

<tensor_type> defines the type (special case or method of description) of tensor. Currently, permitted key words are: CONSTANT_OVERGEN, CONSTANT_UNIAX, CONSTANT_ORTHOROT and TAB_ORTHOROT. These are defined in section 2.6. The list of parameters which follow depend on this key word.

CONSTANT_UNIAX refers to a uniaxial tensor. The list of parameters which follow are:-

< $\Re(a_1)$ > < $\Im(a_1)$ > < $\Re(a_2)$ > < $\Im(a_2)$ > < u_1 > < u_2 > < u_3 >

where $\Re(a_1)$ and $\Im(a_1)$ are real numbers specifying the real and imaginary parts of a_1 , $\Re(a_2)$ and $\Im(a_2)$ are real numbers specifying the real and imaginary parts of a_2 and u_1, u_2 and u_3 are real numbers defining the uniaxial direction vector. These are defined in section 2.6.2.

CONSTANT_ORTHOROT refers to an orthotropic tensor. The list of parameters which follow are:-

< $\Re(\lambda_1)$ > < $\Im(\lambda_1)$ > < $\Re(\lambda_2)$ > < $\Im(\lambda_2)$ > < $\Re(\lambda_3)$ > < $\Im(\lambda_3)$ > < α > < β > < γ >

where $\Re(\lambda_1), \Im(\lambda_1), \Re(\lambda_2), \Im(\lambda_2)$ and $\Re(\lambda_3)$ and $\Im(\lambda_3)$ are real numbers specifying the real and imaginary parts of λ_1, λ_2 and λ_3 respectively. α, β and γ are the (real) Euler angles in degrees. These are defined in section 2.6.3.

TAB_ORTHOROT refers to a tabulated orthotropic tensor with principal components that are frequency dependent. In this case the list of parameters which follow are:-

<tabfile_name> < α > < β > < γ >

where α , β and γ are the (real) Euler angles in degrees. <tabfile_name> is a character string specifying the name of an input file supplying the tabulated data (see below). This is also described in section 2.6.3.

CONSTANT_OVERGEN refers to a general tensor specified by its Cartesian components. The list of parameters which follow are:-

$$\begin{aligned} < \Re(A_{xx}) > < \Im(A_{xx}) > < \Re(A_{xy}) > < \Im(A_{xy}) > < \Re(A_{xz}) > < \Im(A_{xz}) > \backslash \\ < \Re(A_{yx}) > < \Im(A_{yx}) > < \Re(A_{yy}) > < \Im(A_{yy}) > < \Re(A_{yz}) > < \Im(A_{yz}) > \backslash \\ < \Re(A_{zx}) > < \Im(A_{zx}) > < \Re(A_{zy}) > < \Im(A_{zy}) > < \Re(A_{zz}) > < \Im(A_{zz}) > \end{aligned}$$

Here the “\” character is not a program file input; it only has meaning above to signify a line continuation. In the program input file all this data is entered on one line and the real and imaginary parts of A_{**} are specified in the order shown. This is a total of 18 real numbers. The definition of quantities is given in section 2.6.4.

3.2.8 SURFACE

Syntax is:

SURFACE <surface_number> <rotation_angle> <name_1> <name_2>

This is optional. If present, SIGMATYPE key words must also be present which define the principal admittance names 1 and 2. If not present it is assumed there is no admittance surface.

Parameter <surface_number> is an integer $1 \leq i \leq N + 1$ describing the interface number for which the surface is defined, where N is the total number of layers within the composite. Integer 1 specifies the left-most interface, with interface numbers defined sequentially thereafter.

Parameter <rotation_angle> is a real number specifying the rotation angle ν in degrees. This defines the alignment angle associated with the principal admittances.

Parameter <name_1> is a character string specifying the name of the first principal admittance, σ^\perp , defined by the SIGMATYPE key word.

Parameter <name_2> is a character string specifying the name of the second principal admittance, σ^\parallel , defined by the SIGMATYPE key word.

3.2.9 SIGMATYPE

Syntax is:

SIGMATYPE < name > < model_number > { list of parameters }

This key word is mandatory if it is required to define a < name > specified by the SURFACE key word. If no SURFACE key words are present no SIGMATYPE key words are required.

Parameter < name > is a character string which must match <name_1 > or <name_2 > in the SURFACE definition. The SIGMATYPE then defines the referenced admittance.

Parameter < model_number > is an integer that refers to the equivalent circuit model number employed. Currently, as of version 00.03.02 of the software, there are four model types (1,2,3 or 4) defined.

Parameters { list of parameters } are a list of real numbers which specify the equivalent circuit parameters associated with a given model number. These comprise resistances in Ohms, capacitances in pF and inductances in nH.

For model number 1, parameter #1 is R_1 and parameter #2 is L_1 .

For model number 2, parameter #1 is R_1 and parameter #2 is C_1 .

For model number 3, parameter #1 is R_1 , parameter #2 is L_1 and parameter #3 is C_1 .

For model number 4, parameter #1 is R_1 , parameter #2 is L_1 and parameter #3 is C_1 .

3.2.10 Data format for tabulated input file <tabfile_name>

This file is required if the TAB_ORTHOROT option is used on the TENSOR definition. The input file is Fortran free format consisting of a column of frequencies, and three columns of complex numbers. Entry on each row is of the form,

$$< f_v > < \lambda_{1v} > < \lambda_{2v} > < \lambda_{3v} >$$

where f_v is a frequency specified in MHz and λ_{1v} , λ_{2v} and λ_{3v} are those values of λ_1 , λ_2 and λ_3 defined at the frequencies f_v . f_v is a real number, λ_{1v} , λ_{2v} and λ_{3v} are complex numbers. For example, a typical input file specifying λ_i at 7, 9, 10, 12 and 15 GHz might take the form,

7000.0	(3.00,0.00)	(2.00,0.00)	(1.00,0.00)
9000.0	(4.00,0.00)	(3.00,0.00)	(2.00,0.00)
10000.0	(7.00,0.00)	(4.00,0.00)	(2.00,0.00)
12000.0	(4.00,0.00)	(3.00,0.00)	(2.00,0.00)
15000.0	(3.00,0.00)	(2.00,0.00)	(1.00,0.00)

There must be at least three rows. All frequencies must be specified in sequentially increasing order. The minimum and maximum frequencies must lie outside the requested range of frequencies defined by the FREQS tag.

3.3 Output file formats

3.3.1 Format for <filename1>

The first output file specified in the FILENAME definition outputs much of the data shown in the log file. This contains a list of the components of $\underline{\mathcal{T}}$ and $\underline{\mathcal{R}}$ calculated at each angle and frequency. The tilt angles, axial ratios and power balances \mathcal{P}_{TE} and \mathcal{P}_{TM} are also given.

a typical output for a lossless material at two frequencies might look like:

```

-----
theta/deg =    75.0000    phi/deg =    30.0000    frequency/GHz =    8.0000
Transmission and Reflection S-parameters
Index base: (TE_inc TE_out) (TE_inc TM_out)
              (TM_inc TE_out) (TM_inc TM_out)

T(1,1) =    -8.0023 dB        -105.5079 deg        T(1,2) =    -25.2176 dB        129.1274 deg
T(2,1) =   -43.0155 dB        177.5671 deg        T(2,2) =    -1.1096 dB        -134.8070 deg
R(1,1) =    -0.7999 dB        159.3768 deg        R(1,2) =   -21.6687 dB        -57.5728 deg
R(2,1) =   -28.6721 dB        131.8570 deg        R(2,2) =    -6.4963 dB        171.9853 deg

TE Transmission Tilt angle (degrees) =   -85.3825        Axial ratio =    19.0428 dB
TM Transmission Tilt angle (degrees) =     0.3101        Axial ratio =    44.5360 dB
TE Reflection Tilt angle (degrees) =   -85.8520        Axial ratio =    25.3351 dB
TM Reflection Tilt angle (degrees) =     3.4146        Axial ratio =    26.0222 dB
input TE (perpendicular) polarisation balance =    1.0000000
input TM (parallel)      polarisation balance =    1.0000000
-----
theta/deg =    75.0000    phi/deg =    30.0000    frequency/GHz =    9.0000
Transmission and Reflection S-parameters
Index base: (TE_inc TE_out) (TE_inc TM_out)
              (TM_inc TE_out) (TM_inc TM_out)

T(1,1) =    -3.1185 dB        -131.2179 deg        T(1,2) =   -19.7080 dB        48.6547 deg
T(2,1) =   -21.9522 dB        -68.4933 deg        T(2,2) =    -0.8038 dB        -162.0109 deg
R(1,1) =    -3.1780 dB        137.3807 deg        R(1,2) =   -16.8725 dB        -103.5373 deg
R(2,1) =   -18.6051 dB        104.7379 deg        R(2,2) =    -8.2742 dB        152.8164 deg

TE Transmission Tilt angle (degrees) =   -81.5764        Axial ratio =    69.8358 dB
TM Transmission Tilt angle (degrees) =    -0.3104        Axial ratio =    21.1651 dB
TE Reflection Tilt angle (degrees) =   -84.0736        Axial ratio =    14.9551 dB
TM Reflection Tilt angle (degrees) =    12.0733        Axial ratio =    13.2686 dB
input TE (perpendicular) polarisation balance =    1.0000000
input TM (parallel)      polarisation balance =    1.0000000
-----

```

3.3.2 Format for <filename2>

The second output file contains data in column format:-

column 1	frequency in GHz
column 2	theta (θ_{in}) in degrees
column 3	phi (ϕ_{in}) in degrees
columns 4, 5, 6, 7	The square magnitude of the \underline{T} entries $T(1,1)$, $T(1,2)$ $T(2,1)$ and $T(2,2)$ respectively, specified in dB.
columns 8, 9, 10, 11	The phase of the \underline{T} entries $T(1,1)$, $T(1,2)$ $T(2,1)$ and $T(2,2)$ respectively, specified in degrees.
columns 12, 13, 14, 15	The square magnitude of the \underline{R} entries $R(1,1)$, $R(1,2)$ $R(2,1)$ and $R(2,2)$ respectively, specified in dB.
columns 16, 17, 18, 19	The phase of the \underline{R} entries $R(1,1)$, $R(1,2)$ $R(2,1)$ and $R(2,2)$ respectively, specified in degrees.
column 20, 21	The axial ratio associated with TE transmission and TM transmission, respectively.
column 22, 23	The axial ratio associated with TE reflection and TM reflection, respectively.

3.4 Example 1. An anisotropic material for polarisation conversion in free space.

This is an example showing a three layer material which might be used to convert linear to circular polarisation. It is an un-optimised half-wavelength half-wavelength quarter-wavelength design based on the method of Pancharatnam [7]. Note the relative permittivity tensors of the first three layers are rotated in the x-y plane by angles $\alpha = 7^\circ$, 34° and 100° respectively. The input file is given by:-

```

STRUCTURE 3 FREE 1 2 3
FILENAME output1.dat output2.dat
ANGLES 00.0 0.0 1 00.0 0.0 1
FREQS 5000.0 200.0 100

MATERIAL 1 0.0200 epsname1 muname1 xiname1 zetaname1
MATERIAL 2 0.0200 epsname2 muname1 xiname1 zetaname1
MATERIAL 3 0.0100 epsname3 muname1 xiname1 zetaname1

TENSOR epsname1 CONSTANT_ORTHOROT 3.0, 0.0 1.5, 0.0 3.0, 0.0 07.0,0.0,0.0
TENSOR epsname2 CONSTANT_ORTHOROT 3.0, 0.0 1.5, 0.0 3.0, 0.0 34.0,0.0,0.0
TENSOR epsname3 CONSTANT_ORTHOROT 3.0, 0.0 1.5, 0.0 3.0, 0.0 100.0,0.0,0.0
TENSOR muname1 CONSTANT_OVERGEN 1.0,-0.0 0.0,0.0 0.0,0.0 0.0,0.0 1.0,-0.0 0.0,0.0 \
0.0,0.0 0.0,0.0 1.0,0.0
TENSOR xiname1 CONSTANT_OVERGEN 0.0,0.0 0.0,0.0 0.0,0.0 0.0,0.0 0.0,0.0 0.0,-0.0 \
0.0,0.0 0.0,0.0 0.0,-0.0
TENSOR zetaname1 CONSTANT_OVERGEN 0.0,0.0 0.0,0.0 0.0,0.0 0.0,0.0 0.0,0.0 0.0,0.0 \
0.0,0.0 0.0,0.0 0.0,-0.0

```

where the \ character is not a program input; this is shown to represent an extended line in the report.

The program generates sets of data for 100 frequencies so only the first two output blocks of the file *output1.dat* are shown. These are:-

```
-----
theta/deg =      0.0000  phi/deg =      0.0000  frequency/GHz =      5.0000
Transmission and Reflection S-parameters
Index base: (TE_inc TE_out) (TE_inc TM_out)
             (TM_inc TE_out) (TM_inc TM_out)

T(1,1) =      -1.8248 dB      -55.2175 deg      T(1,2) =      -6.9283 dB      -135.6844 deg
T(2,1) =      -7.4916 dB      150.0044 deg      T(2,2) =      -1.7514 dB      -115.5389 deg
R(1,1) =      -9.4555 dB      -104.9085 deg      R(1,2) =     -15.7090 dB      -59.4733 deg
R(2,1) =     -15.7090 dB      120.5267 deg      R(2,2) =      -8.9675 dB      27.9675 deg

TE Transmission Tilt angle (degrees) =      82.5445      Axial ratio =      5.3282 dB
TM Transmission Tilt angle (degrees) =      -3.1228      Axial ratio =      5.7854 dB
TE Reflection Tilt angle (degrees) =      69.0810      Axial ratio =     10.2641 dB
TM Reflection Tilt angle (degrees) =      -1.4923      Axial ratio =      6.7547 dB
input TE (perpendicular) polarisation balance =      1.0000000
input TM (parallel)      polarisation balance =      1.0000000
-----
theta/deg =      0.0000  phi/deg =      0.0000  frequency/GHz =      5.2000
Transmission and Reflection S-parameters
Index base: (TE_inc TE_out) (TE_inc TM_out)
             (TM_inc TE_out) (TM_inc TM_out)

T(1,1) =      -2.0506 dB      -71.1225 deg      T(1,2) =      -6.5287 dB      -151.4798 deg
T(2,1) =      -7.3768 dB      132.0308 deg      T(2,2) =      -1.9227 dB      -133.9821 deg
R(1,1) =      -8.6690 dB      -128.4056 deg      R(1,2) =     -17.4242 dB      -87.3265 deg
R(2,1) =     -17.4242 dB      92.6735 deg      R(2,2) =      -8.0499 dB      16.2605 deg

TE Transmission Tilt angle (degrees) =      81.3639      Axial ratio =      4.7327 dB
TM Transmission Tilt angle (degrees) =      -2.9624      Axial ratio =      5.4918 dB
TE Reflection Tilt angle (degrees) =      73.7973      Axial ratio =     13.0706 dB
TM Reflection Tilt angle (degrees) =      5.1166      Axial ratio =      9.6827 dB
input TE (perpendicular) polarisation balance =      1.0000000
input TM (parallel)      polarisation balance =      1.0000000
```


The first 8 columns of the file *output2.dat* are shown below:-

freq/GHz	theta/deg	phi/deg	t_11(db)	t_12(db)	t_21(db)	t_22(db)	t_11(deg)	...
5.00000	0.00000	0.00000	-1.8248	-6.9283	-7.4916	-1.7514	-55.2175	...
5.20000	0.00000	0.00000	-2.0506	-6.5287	-7.3768	-1.9227	-71.1225	...
5.40000	0.00000	0.00000	-2.2404	-6.1519	-7.1477	-2.0157	-86.4358	...
5.60000	0.00000	0.00000	-2.3501	-5.8632	-6.7908	-2.0322	-101.3389	...

When plotted by third party software, the \mathcal{T}_{11} , \mathcal{T}_{12} (linear co and-cross polar transmitted power coefficients associated with an incident TE (\perp) wave) and the axial ratio associated with the incident TE wave are illustrated in figure 3-1. Since this is normal incidence the wave is also TM. The component shown is for an incident wave polarised in the \hat{e}_{\perp} direction which for $\phi = 0$ is y-polarised.

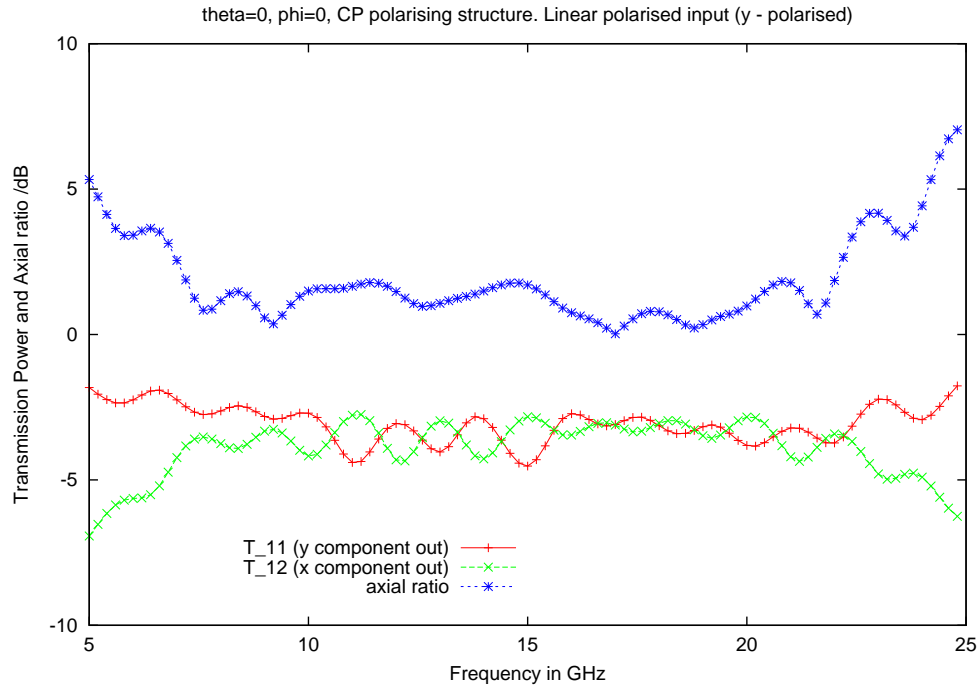


Figure 3-1: Output powers and axial ratio for a y-polarised incident wave

3.5 Example 2. An anisotropic radome composite in free space.

In this example we replicate Rikte et al's example 8.2 of [1]. This represents an anisotropic 3-layer radome structure comprising an ABA structure with Epoxy/E-glass skins over a low density Rohacell. The input file is given by,

```
STRUCTURE 3 FREE 1 2 3
FILENAME output2a.dat output2b.dat
ANGLES 00.0 15.0 6 0.0 0.0 1
FREQS 500.0 500.0 81

MATERIAL 1 0.0008 epoxy_eglass muname1 xiname1 zetaname1
MATERIAL 2 0.0064 rohacell muname1 xiname1 zetaname1
MATERIAL 3 0.0008 epoxy_eglass muname1 xiname1 zetaname1

TENSOR epoxy_eglass CONSTANT_OVERGEN 4.444,-0.096792 0.0, 0.0 0.0, 0.0 \
0.000, 0.0 4.444,-0.096792 0.0, 0.0 \
0.000, 0.0 0.0, 0.0 4.23,-0.104904
TENSOR rohacell CONSTANT_OVERGEN 1.10,-0.00044 0.0, 0.0 0.0, 0.0 \
0.00, 0.0 1.10,-0.00044 0.0, 0.0 \
0.00, 0.0 0.0, 0.0 1.10,-0.00044
TENSOR muname1 CONSTANT_OVERGEN 1.00,-0.0 0.0, 0.0 0.0, 0.0 \
0.0, 0.0 1.0, -0.0 0.0, 0.0 \
0.0, 0.0 0.0, 0.0 1.0, -0.0
TENSOR xiname1 CONSTANT_OVERGEN 0.0,0.0 0.0,0.0 0.0,0.0 \
0.0,0.0 0.0,0.0 0.0,0.0 \
0.0,0.0 0.0,0.0 0.0,0.0
TENSOR zetaname1 CONSTANT_OVERGEN 0.0,0.0 0.0,0.0 0.0,0.0 \
0.0,0.0 0.0,0.0 0.0,0.0 \
0.0,0.0 0.0,0.0 0.0,0.0
```

where, as above, the “\” symbol just signifies a line continuation for illustration purposes and is not present in the actual input file (where each continued data set appears on the same line). The first two blocks of the output file “output2a.dat” are given below. The TE and TM plotted data are illustrated in figures 3-2 and 3-3 below, using the same scales as in [1]. As far as we can tell the results appear to be the same.

```

-----
theta/deg =      0.0000   phi/deg =      0.0000   frequency/GHz =      0.5000
Transmission and Reflection S-parameters
Index base: (TE_inc TE_out) (TE_inc TM_out)
             (TM_inc TE_out) (TM_inc TM_out)

T(1,1) =      -0.0116 dB      -6.6453 deg      T(1,2) =     -300.0000 dB      0.0000 deg
T(2,1) =     -300.0000 dB      0.0000 deg      T(2,2) =      -0.0116 dB     -6.6453 deg
R(1,1) =     -29.8785 dB     -98.1118 deg      R(1,2) =     -300.0000 dB      0.0000 deg
R(2,1) =     -300.0000 dB      0.0000 deg      R(2,2) =     -29.8785 dB     81.8882 deg

TE Transmission Tilt angle (degrees) =    -90.0000      Axial ratio =    418.7200 dB
TM Transmission Tilt angle (degrees) =      0.0000      Axial ratio =    418.7200 dB
TE Reflection Tilt angle (degrees)   =    -90.0000      Axial ratio =    370.2088 dB
TM Reflection Tilt angle (degrees)   =      0.0000      Axial ratio =    370.2088 dB
input TE (perpendicular) polarisation balance =      0.9983561
input TM (parallel)      polarisation balance =      0.9983561
-----
theta/deg =      0.0000   phi/deg =      0.0000   frequency/GHz =      1.0000
Transmission and Reflection S-parameters
Index base: (TE_inc TE_out) (TE_inc TM_out)
             (TM_inc TE_out) (TM_inc TM_out)

T(1,1) =      -0.0316 dB     -13.2706 deg      T(1,2) =     -300.0000 dB      0.0000 deg
T(2,1) =     -300.0000 dB      0.0000 deg      T(2,2) =      -0.0316 dB     -13.2706 deg
R(1,1) =     -23.9798 dB     -104.7306 deg      R(1,2) =     -300.0000 dB      0.0000 deg
R(2,1) =     -300.0000 dB      0.0000 deg      R(2,2) =     -23.9798 dB     75.2694 deg

TE Transmission Tilt angle (degrees) =    -90.0000      Axial ratio =    412.7509 dB
TM Transmission Tilt angle (degrees) =      0.0000      Axial ratio =    412.7509 dB
TE Reflection Tilt angle (degrees)   =    -90.0000      Axial ratio =    376.3105 dB
TM Reflection Tilt angle (degrees)   =      0.0000      Axial ratio =    376.3105 dB
input TE (perpendicular) polarisation balance =      0.9967513
input TM (parallel)      polarisation balance =      0.9967513
-----

```

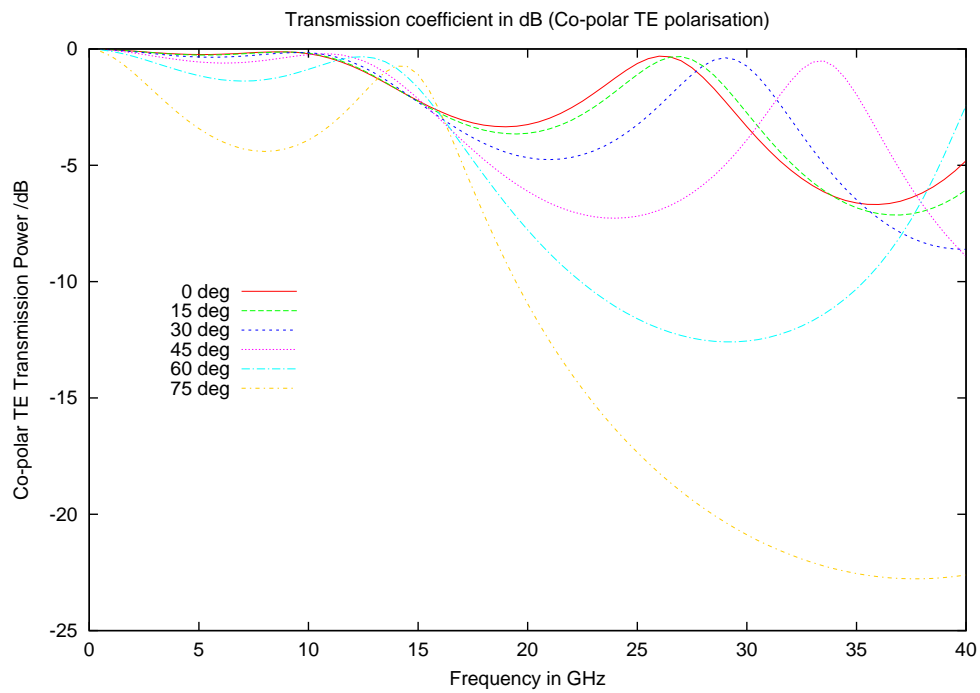


Figure 3-2: Co-polar Transmission for incident TE waves

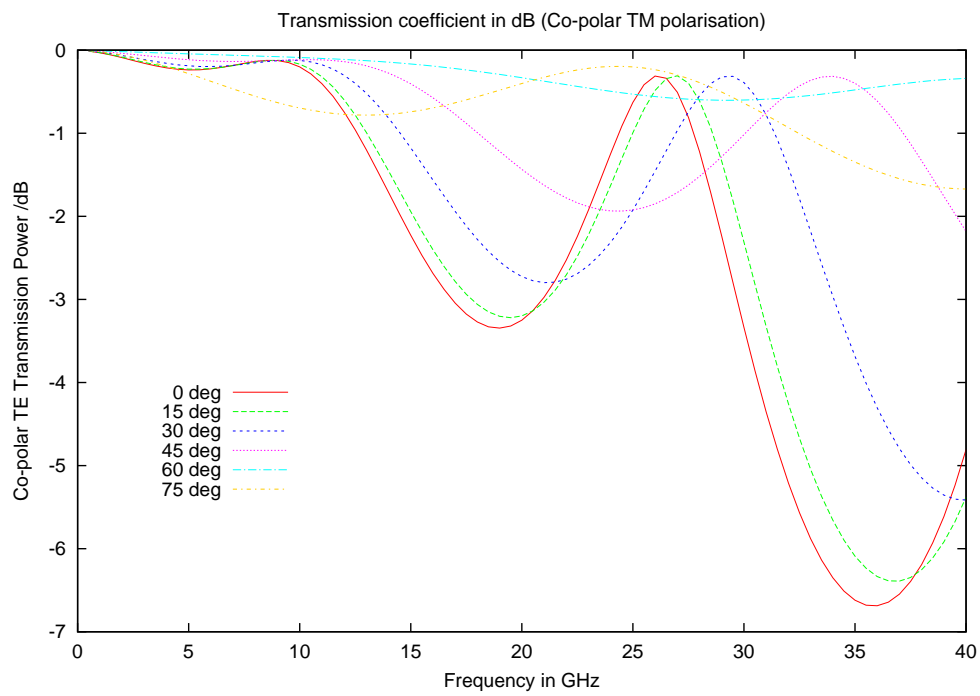


Figure 3-3: Co-polar Transmission for incident TM waves

3.6 Example 3. A bianisotropic material in free space.

In this example we replicate Rikte et al's example 8.3 of [1]. This represents a bianisotropic single layer structure employed as a model of an Ω -material.

```
STRUCTURE 1 FREE 1
FILENAME output3a.dat output3b.dat
ANGLES 00.0 2.0 45 0.0 2.0 46
FREQS 10000.0 00.0 1
MATERIAL 1 0.030 epsname1 muname1 xiname1 zetaname1
TENSOR epsname1 CONSTANT_OVERGEN 3.0,-0.0 0.0,0.0 0.0,0.0 \
                                0.0,0.0 5.0,0.0 0.0,0.0 \
                                0.0,0.0 0.0,0.0 3.0,0.0
TENSOR muname1 CONSTANT_OVERGEN 1.0,-0.0 0.0,0.0 0.0,0.0 \
                                0.0,0.0 1.0,0.0 0.0,0.0 \
                                0.0,0.0 0.0,0.0 1.1,0.0
TENSOR xiname1 CONSTANT_OVERGEN 0.0,0.0 0.0,0.0 0.0,0.0 \
                                0.0,0.0 0.0,0.0 0.0,-0.5 \
                                0.0,0.0 0.0,0.0 0.0,0.0
TENSOR zetaname1 CONSTANT_OVERGEN 0.0,0.0 0.0,0.0 0.0,0.0 \
                                0.0,0.0 0.0,0.0 0.0,0.0 \
                                0.0,0.0 0.0,0.5 0.0,0.0
```

As above the “\” syntax is used just to identify a line continuation. Also note that the non-zero entries in the ξ and ζ tensors are imaginary and are thus of opposite sign to that employed in example 8.3 of [1] due to the alternative $i \rightarrow -j$ harmonic sign convention, as described in the introduction of this report.

The first two blocks of the output file *output3a.dat* are given below:-

```

-----
theta/deg =      0.0000   phi/deg =      0.0000   frequency/GHz =      10.0000
Transmission and Reflection S-parameters
Index base: (TE_inc TE_out) (TE_inc TM_out)
              (TM_inc TE_out) (TM_inc TM_out)

T(1,1) =      -2.1270 dB          -72.2058 deg          T(1,2) =     -300.0000 dB          0.0000 deg
T(2,1) =     -300.0000 dB           0.0000 deg          T(2,2) =       -1.2374 dB          95.2271 deg
R(1,1) =       -4.1203 dB          -162.2058 deg          R(1,2) =     -300.0000 dB          0.0000 deg
R(2,1) =     -300.0000 dB           0.0000 deg          R(2,2) =       -6.0568 dB          5.2271 deg

TE Transmission Tilt angle (degrees) =    -90.0000      Axial ratio =    398.2988 dB
TM Transmission Tilt angle (degrees) =      0.0000      Axial ratio =    398.7988 dB
TE Reflection Tilt angle (degrees) =     -90.0000      Axial ratio =    406.1766 dB
TM Reflection Tilt angle (degrees) =      0.0000      Axial ratio =    414.7526 dB
input TE (perpendicular) polarisation balance =      1.0000000
input TM (parallel)      polarisation balance =      1.0000000
-----

theta/deg =      0.0000   phi/deg =      2.0000   frequency/GHz =      10.0000
Transmission and Reflection S-parameters
Index base: (TE_inc TE_out) (TE_inc TM_out)
              (TM_inc TE_out) (TM_inc TM_out)

T(1,1) =      -2.1491 dB          -72.1889 deg          T(1,2) =     -24.8513 dB          101.1878 deg
T(2,1) =     -24.8513 dB          101.1878 deg          T(2,2) =       -1.2573 dB          95.2133 deg
R(1,1) =       -4.1226 dB          -162.2179 deg          R(1,2) =     -44.3328 dB          -123.7232 deg
R(2,1) =     -44.3328 dB           56.2768 deg          R(2,2) =       -6.0545 dB           5.2460 deg

TE Transmission Tilt angle (degrees) =    -85.8374      Axial ratio =     41.5085 dB
TM Transmission Tilt angle (degrees) =      3.7623      Axial ratio =     43.2836 dB
TE Reflection Tilt angle (degrees) =      89.5623      Axial ratio =     44.3287 dB
TM Reflection Tilt angle (degrees) =      0.4394      Axial ratio =     40.4651 dB
input TE (perpendicular) polarisation balance =      1.0000000
input TM (parallel)      polarisation balance =      1.0000000
-----

```

Excitation is with a plane wave at a single frequency where the material is exactly one wavelength thick ($k_0 d = 2\pi$). Three dimensional plots are given of the total transmitted power as a function of both θ_{in} and ϕ_{in} for the TE and TM polarisations. These are defined, in our notation, by

$$\begin{aligned}
 T_{TE} &= |T_{11}|^2 + |T_{12}|^2 \\
 T_{TM} &= |T_{21}|^2 + |T_{22}|^2
 \end{aligned} \tag{3-1}$$

These are shown in figures 3-4 and 3-5 and appear to agree well with the figure 8 predictions of [1]. The results actually differ little from results (not shown) when $\xi = \zeta = 0$, except for angles approaching grazing incidence.

TE transmission (total power) coefficient linear power scale

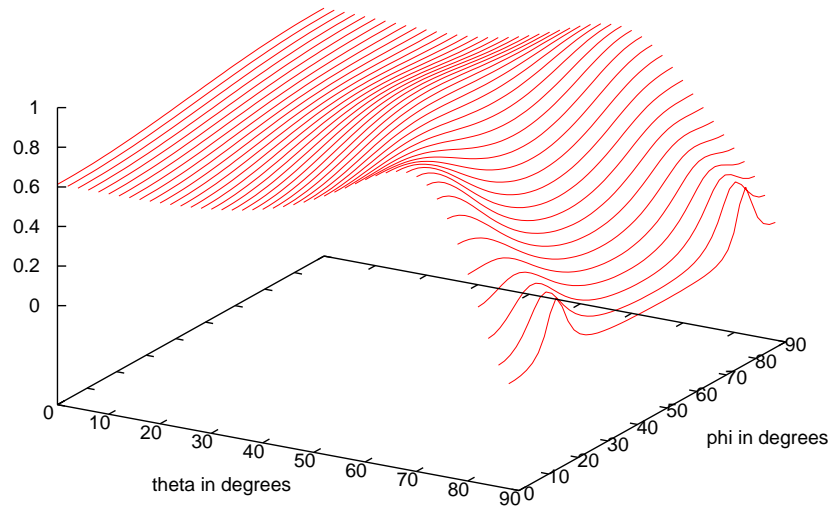


Figure 3-4: Transmittance T_{TE} for incident TE waves (linear scale)

TM transmission (total power) coefficient linear power scale

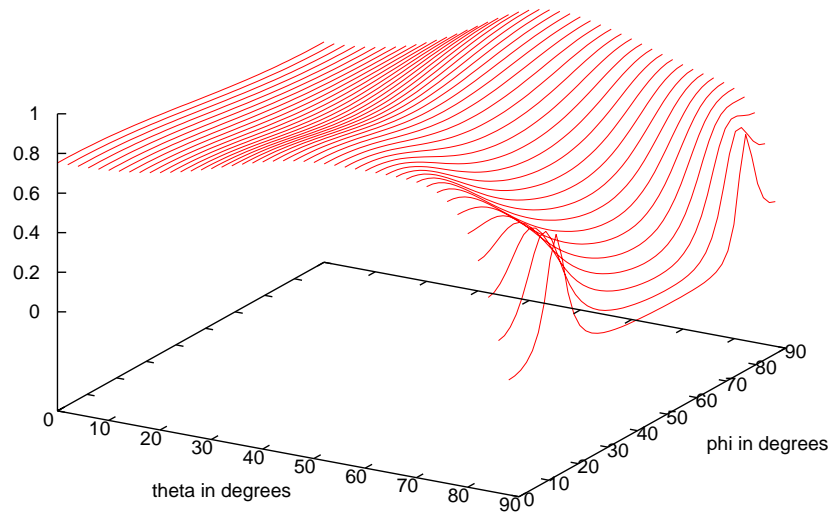


Figure 3-5: Transmittance T_{TM} for incident TE waves (linear scale)

3.7 Example 4. An anisotropic RAM.

In this example we consider a three layer radar absorbing material (RAM), using the PEC termination option. It is taken to include some anisotropy, and a small non-unity relative permeability, but is not intended to represent any particular synthesised material. Also note that a constant valued lossy relative permittivity or permeability is not realisable, though it is often used as an approximation over a limited bandwidth. The input file is given as :-

```
STRUCTURE 3 PEC 1 2 3
FILENAME output1.dat output2.dat
ANGLES 00.0 15.0 5 00.0 0.0 1
FREQS 200.0 200.0 130

MATERIAL 1 0.0100 epsname1 muname1 xiname1 zetaname1
MATERIAL 2 0.0100 epsname2 muname1 xiname1 zetaname1
MATERIAL 3 0.0100 epsname3 muname1 xiname1 zetaname1

TENSOR epsname1 CONSTANT_ORTHOROT 1.1, -0.3 1.1, -0.3 1.2, -0.4 0.0,0.0,0.0
TENSOR epsname2 CONSTANT_ORTHOROT 1.3, -0.4 1.3, -0.4 1.5, -0.6 0.0,0.0,0.0
TENSOR epsname3 CONSTANT_ORTHOROT 1.5, -0.6 1.5, -0.6 1.8, -0.8 0.0,0.0,0.0
TENSOR muname1 CONSTANT_OVERGEN 1.3,-0.1 0.0,0.0 0.0,0.0 \
                                0.0,0.0 1.3,-0.1 0.0,0.0 \
                                0.0,0.0 0.0,0.0 1.3,-0.1
TENSOR xiname1 CONSTANT_OVERGEN 0.0,0.0 0.0,0.0 0.0,0.0 \
                                0.0,0.0 0.0,0.0 0.0,-0.0 \
                                0.0,0.0 0.0,0.0 0.0,0.0
TENSOR zetaname1 CONSTANT_OVERGEN 0.0,0.0 0.0,0.0 0.0,0.0 \
                                0.0,0.0 0.0,0.0 0.0,0.0 \
                                0.0,0.0 0.0,0.0 0.0,0.0
```

As in previous examples the \ symbol is used to indicate line continuation. A section of data from the file “*output1.dat*” is given here:-

```
-----
theta/deg = 60.0000 phi/deg = 0.0000 frequency/GHz = 2.0000
Transmission and Reflection S-parameters
Index base: (TE_inc TE_out) (TE_inc TM_out)
            (TM_inc TE_out) (TM_inc TM_out)

T(1,1) = -300.0000 dB          0.0000 deg          T(1,2) = -300.0000 dB          0.0000 deg
T(2,1) = -300.0000 dB          0.0000 deg          T(2,2) = -300.0000 dB          0.0000 deg
R(1,1) = -5.5878 dB          79.1200 deg          R(1,2) = -300.0000 dB          0.0000 deg
R(2,1) = -300.0000 dB          0.0000 deg          R(2,2) = -4.0971 dB          -163.9202 deg

TE Transmission Tilt angle (degrees) = -45.0000          Axial ratio = 324.2607 dB
TM Transmission Tilt angle (degrees) = -45.0000          Axial ratio = 324.2607 dB
TE Reflection Tilt angle (degrees) = 90.0000          Axial ratio = 394.5698 dB
TM Reflection Tilt angle (degrees) = 0.0000          Axial ratio = 407.0541 dB
input TE (perpendicular) polarisation balance = 0.2762002
input TM (parallel) polarisation balance = 0.3893059
-----
```


The transmission coefficient for a PEC backed structure is defined as zero, which in dB terms is assigned a finite number (-300 dB). The axial ratios and tilt angles attributed to transmission are similarly ill-defined in this instance, but are assigned numerical values without causing software faults.

Figures 3-6 and 3-7 show the co-polar TE and TM reflection coefficients as a function of frequency and incidence angle. This example predicts that deliberate use of anisotropy has the potential to equalise the TE and TM reflection coefficients as the angle of incidence is changed. Often, and this is the case here, if the materials are isotropic there is an increasing divergence between TE and TM results as θ_{in} is increased.

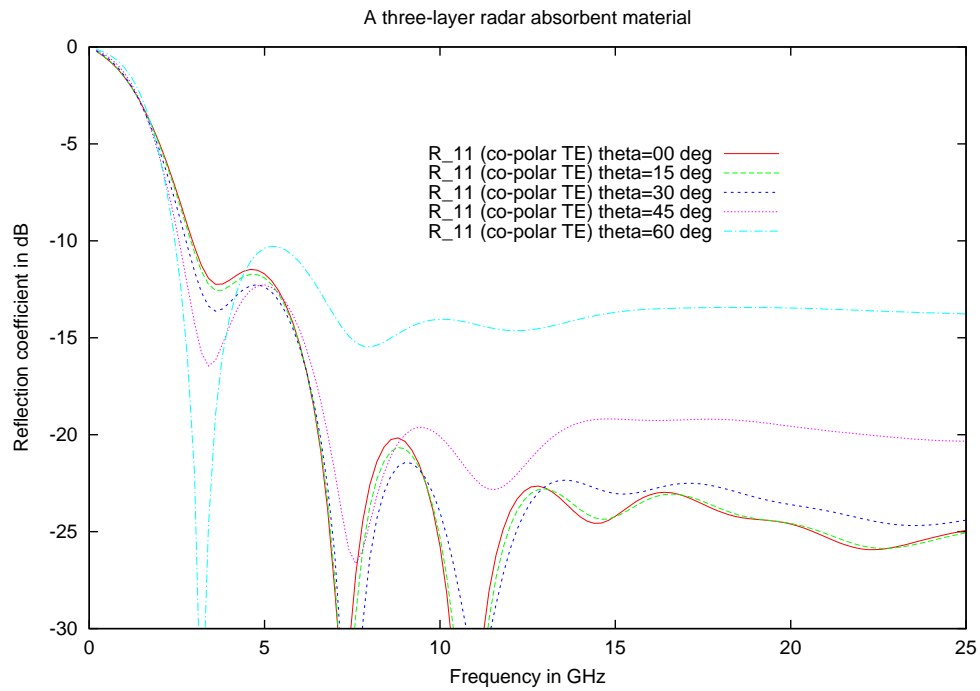


Figure 3-6: Co-polar Reflection for incident TE waves

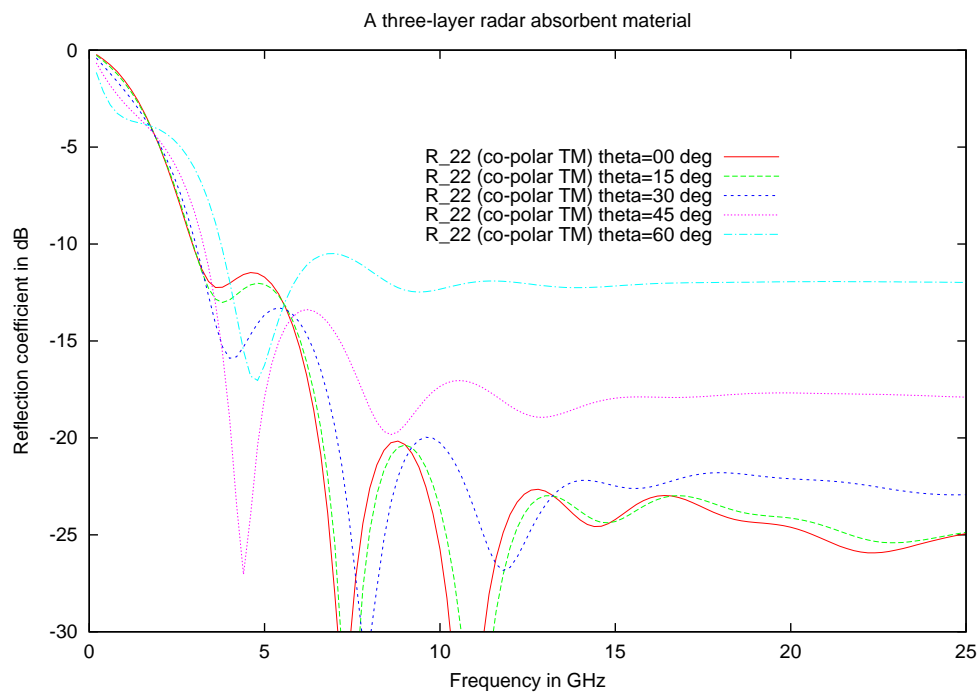


Figure 3-7: Co-polar Reflection for incident TM waves

3.8 Example 5. A new kind of reflection polariser.

In this example we have used the software to explore a possibility for designing a linear-to-circular polariser that operates in *reflection* over an octave bandwidth. To our knowledge there are currently no analytical methods (unlike the transmission mode device [7]) for the design of wide band polarisers of this type, but we expect a number of possible applications for high power reflector antennas.

It would appear that an (A)(B)(A/2) structure, backed by a perfect conductor, shows good performance. This is a structure, as sketched in figure 3-8, where each layer is anisotropic in the xy plane, co-aligned and rotated 45° to the incident linearly polarised wave.

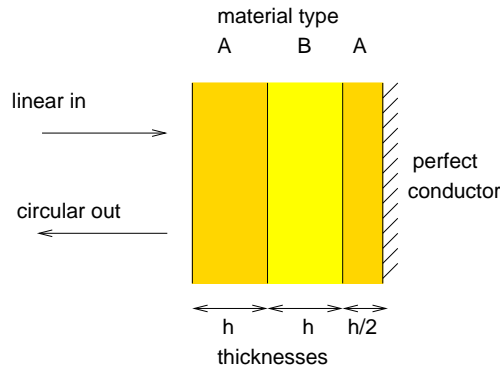


Figure 3-8: An ABA/2 PEC terminated structure for the design of a reflector polariser (linear to circular)

The input file shown below represents a material with $h = 22$ mm. Material A has $\epsilon_{xx} = \epsilon_{zz} = 2.6$ and $\epsilon_{yy} = 1.5$. Material B has $\epsilon_{xx} = \epsilon_{zz} = 3.0$ and $\epsilon_{yy} = 1.5$. The materials are then rotated by 45° about the z-axis. Input file is:-

```
STRUCTURE 3 PEC 1 2 3
FILENAME output1.dat output2.dat
ANGLES 00.0 0.0 1 00.0 0.0 1
FREQS 5000.0 200.0 100

MATERIAL 1 0.0022 epsname1 muname1 xiname1 zetaname1
MATERIAL 2 0.0022 epsname2 muname1 xiname1 zetaname1
MATERIAL 3 0.0011 epsname3 muname1 xiname1 zetaname1

TENSOR epsname1 CONSTANT_ORTHOROT 2.6, 0.0 1.5, 0.0 2.6, 0.0 45.0,0.0,0.0
TENSOR epsname2 CONSTANT_ORTHOROT 3.0, 0.0 1.5, 0.0 3.0, 0.0 45.0,0.0,0.0
TENSOR epsname3 CONSTANT_ORTHOROT 2.6, 0.0 1.5, 0.0 2.6, 0.0 45.0,0.0,0.0
```

```

    TENSOR muname1 CONSTANT_OVERGEN  1.0,-0.0  0.0,0.0  0.0,0.0  \
                                     0.0,0.0  1.0,-0.0  0.0,0.0  \
                                     0.0,0.0  0.0,0.0  1.0,-0.0
    TENSOR xiname1 CONSTANT_OVERGEN  0.0,0.0  0.0,0.0  0.0,0.0  \
                                     0.0,0.0  0.0,0.0  0.0,-0.0  \
                                     0.0,0.0  0.0,0.0  0.0,0.0
    TENSOR zetaname1 CONSTANT_OVERGEN 0.0,0.0  0.0,0.0  0.0,0.0  \
                                     0.0,0.0  0.0,0.0  0.0,0.0  \
                                     0.0,0.0  0.0,0.0  0.0,0.0

```

The predicted reflection coefficients (co- and cross-polar) and the axial ratio are shown in figure 3-9 below. The axial ratio is less than 1dB over the octave.

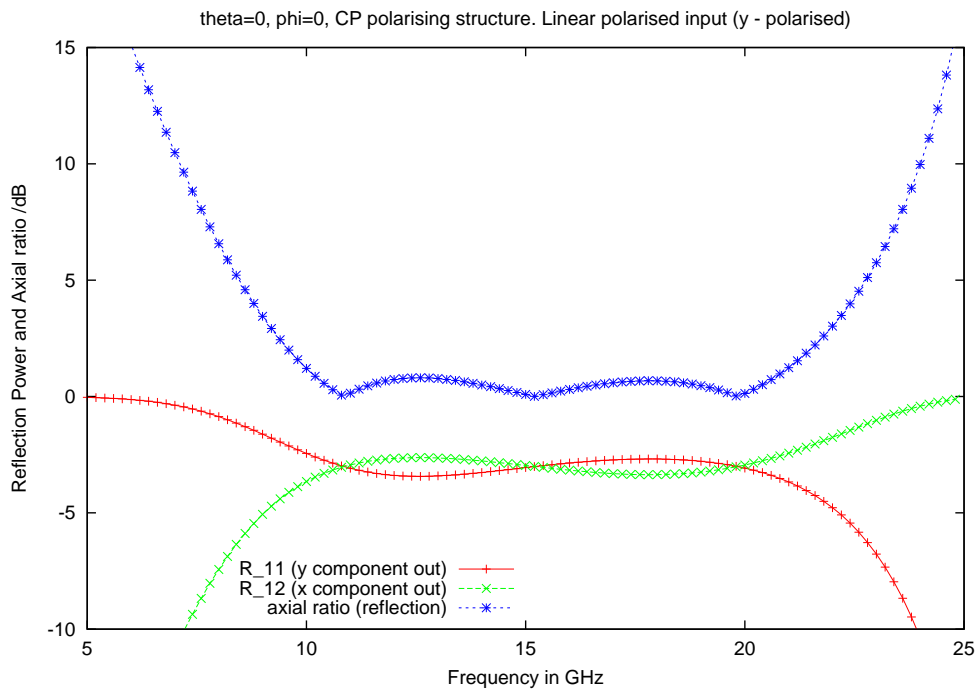


Figure 3-9: Output powers and axial ratio for a y-polarised incident wave

3.9 Example 6. A sheet polariser showing the problem with formulation 1

In this example we illustrate why there is a need to employ the more complicated second formulation of section 2.4 rather than the first formulation of section 2.3 when the structure comprises five low resistance (five ohm) thin polarising grids in free space. The input file is given by,

```
STRUCTURE 5 FREE 1 2 3 4 5
FILENAME output1.dat output2.dat
ANGLES 00.0 00.0 1 00.0 0.0 1
FREQS 500.0 500.0 100

MATERIAL 3 0.0030 epsname0 muname0 xiname1 zetaname1
MATERIAL 4 0.0030 epsname0 muname0 xiname1 zetaname1
MATERIAL 5 0.0030 epsname0 muname0 xiname1 zetaname1
MATERIAL 1 0.0030 epsname0 muname0 xiname1 zetaname1
MATERIAL 2 0.0030 epsname1 muname1 xiname1 zetaname1

TENSOR epsname0 CONSTANT_ORTHOROT 1.0, 0.0 1.0, 0.0 1.0, 0.0 0.0,0.0,0.0
TENSOR epsname1 CONSTANT_ORTHOROT 1.0, 0.0 1.0, 0.0 1.0, 0.0 0.0,0.0,0.0
TENSOR muname0 CONSTANT_ORTHOROT 1.0,-0.0 1.0, 0.0 1.0, 0.0 0.0,0.0,0.0
TENSOR muname1 CONSTANT_ORTHOROT 1.0,-0.0 1.0, 0.0 1.0, 0.0 0.0,0.0,0.0
TENSOR xiname1 CONSTANT_ORTHOROT 0.0, 0.0 0.0, 0.0 0.0, 0.0 0.0,0.0,0.0
TENSOR zetaname1 CONSTANT_ORTHOROT 0.0, 0.0 0.0, 0.0 0.0, 0.0 0.0,0.0,0.0

SURFACE 1 04.0 sigma1 sigma2
SURFACE 2 10.0 sigma1 sigma2
SURFACE 3 22.5 sigma1 sigma2
SURFACE 4 35.0 sigma1 sigma2
SURFACE 5 41.0 sigma1 sigma2
SURFACE 6 45.0 sigma1 sigma2

SIGMATYPE sigma1 1 1.0e+08 0.0
SIGMATYPE sigma2 1 5.0 0.00
```

Figures 3-10 and 3-11 show the predicted transmission coefficients using the first and second formulations. The ill-conditioning leads to incorrect predictions with formulation 1 as is clear from the figures. The ill-conditioning becomes worse the smaller the resistance value defined for *sigma2* in the first formulation. The second formulation remains stable for very small values (currently limited in the surface impedance definition to 0.001 Ohms).

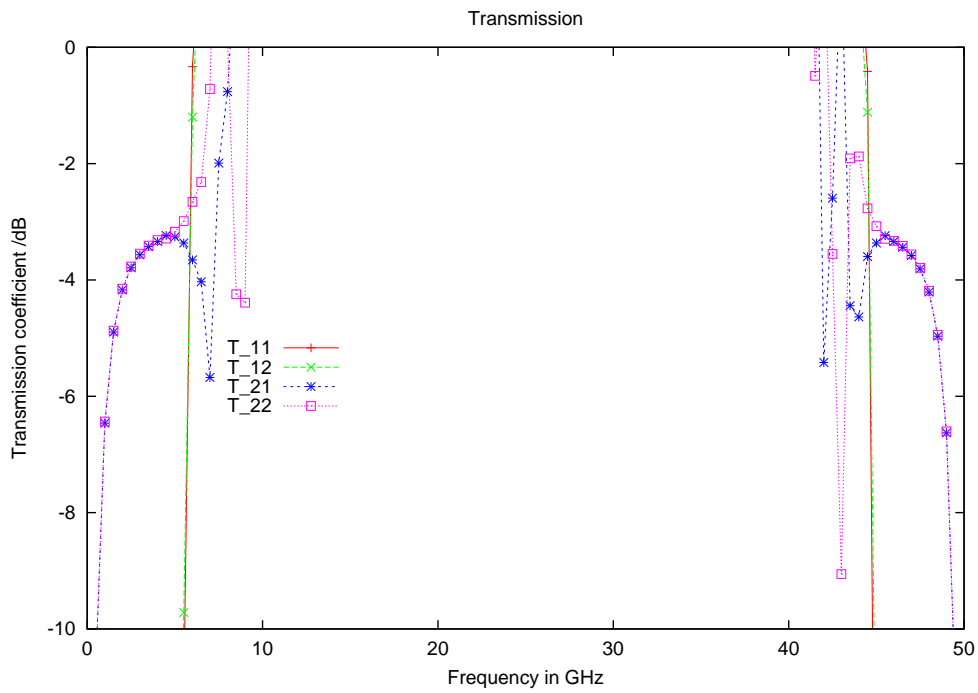


Figure 3-10: Transmission coefficients for a 45 degree polariser using software version 00.02.00 and ill-conditioning (formulation 1).

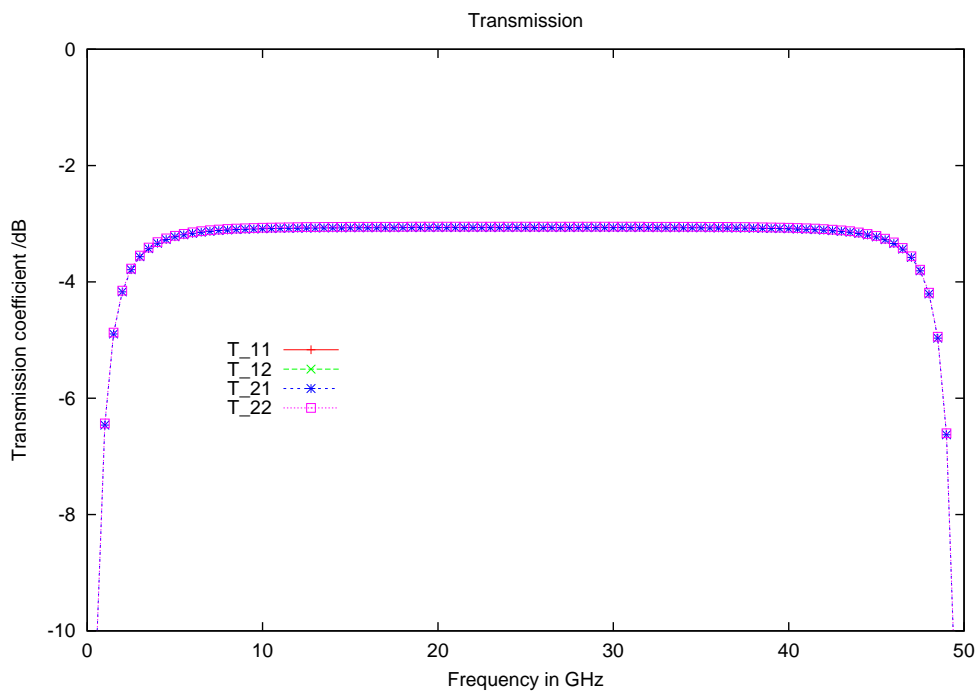


Figure 3-11: Transmission coefficients for a 45 degree polariser using software version 00.03.02 and no ill-conditioning (formulation 2).

3.10 Example 7. Optimised 4-sheet polarisers using formulation 2.

In this example we use the second formulation within a simplex optimiser⁹ where a certain degree of robustness is required. The structure pre-supposes three layers of low dielectric constant foam ($\epsilon_r = 1.1$) with four idealised polarising grids, angled differently on each interface. The layers are each 3.2 mm thick with a frequency range nominally between 2 and 42 GHz. Analysis is conducted at normal incidence.

The angle ν , for the fourth interface is fixed at 45 degrees, while the other three values of ν are controlled by the optimiser. Two examples, 7a and 7b, are given using different cost functions. The input files, after optimisation, are presented where the frequency range is used to control the cost function. Once optimised, the frequency range in the input files is extended to present results between 0.2 and 45 GHz.

3.10.1 Example 7a

In this case, an optimiser cost function is defined as the minimum total transmitted power ($\mathcal{T}_{21} + \mathcal{T}_{22}$, expressed as a power, not in dB) over the defined frequency interval and we wish to maximise this quantity as a function of the angles ν_1 , ν_2 and ν_3 . The frequency interval is from 1.6 GHz to 41.6 GHz. The final input file, after optimisation, is given by,

```
STRUCTURE 3 FREE 1 2 3
FILENAME output1.dat output2.dat
ANGLES 00.0 0.0 1 00.0 0.0 1
FREQS 1600.0 200.0 201
MATERIAL 1 0.0032 epsname1 muname1 xiname1 zetaname1
MATERIAL 2 0.0032 epsname2 muname1 xiname1 zetaname1
MATERIAL 3 0.0032 epsname3 muname1 xiname1 zetaname1
TENSOR epsname1 CONSTANT_ORTHOROT 1.1 0.0 1.1 0.0 1.1 0.0 00.0 0.0 0.0
TENSOR epsname2 CONSTANT_ORTHOROT 1.1 0.0 1.1 0.0 1.1 0.0 00.0 0.0 0.0
TENSOR epsname3 CONSTANT_ORTHOROT 1.1 0.0 1.1 0.0 1.1 0.0 00.0 0.0 0.0
TENSOR muname1 CONSTANT_OVERGEN 1.0 -0.0 0.0 0.0 0.0 0.0 0.0 0.0 1.0 \
                                -0.0 0.0 0.0 0.0 0.0 0.0 0.0 1.0 -0.0
TENSOR xiname1 CONSTANT_OVERGEN 0.0 0.0 0.0 0.0 0.0 0.0 0.0 0.0 0.0 \
                                0.0 0.0 -0.0 0.0 0.0 0.0 0.0 0.0 0.0
TENSOR zetaname1 CONSTANT_OVERGEN 0.0 0.0 0.0 0.0 0.0 0.0 0.0 0.0 0.0 \
                                0.0 0.0 0.0 0.0 0.0 0.0 0.0 0.0 0.0
SURFACE 1 0.202284E+02 sigma1 sigma2
SURFACE 2 0.285053E+02 sigma1 sigma2
SURFACE 3 0.366852E+02 sigma1 sigma2
SURFACE 4 45.0 sigma1 sigma2
SIGMATYPE sigma1 1 1.0e+08 0.0
SIGMATYPE sigma2 1 0.00 0.0
```

⁹Using in-house software “optimiz”.

Note that the optimum grid angles are approximately 20.2° , 28.5° , 36.7° and the pre-defined 45° . Plots showing the reflectivities and transmissivities in dB are given in figures 3-12 and 3-13. These angles are principally controlled by the requirement for best performance at the top and bottom of the frequency interval.

3.10.2 Example 7b

In this case, an optimiser cost function is defined as the maximum total reflected power orthogonal to the incident principal polarisation, \mathcal{R}_{22} (expressed as a power, not in dB) over the defined frequency interval and we wish to minimise this quantity as a function of the angles ν_1 , ν_2 and ν_3 . The frequency interval is from 4.0 GHz to 40.6 GHz. The final input file, after optimisation, is given by,

```

STRUCTURE 3 FREE 1 2 3
FILENAME output1.dat output2.dat
ANGLES 00.0 0.0 1 00.0 0.0 1
FREQS 4000.0 200.0 184
MATERIAL 1 0.0032 epsname1 muname1 xiname1 zetaname1
MATERIAL 2 0.0032 epsname2 muname1 xiname1 zetaname1
MATERIAL 3 0.0032 epsname3 muname1 xiname1 zetaname1
TENSOR epsname1 CONSTANT_ORTHOROT 1.1 0.0 1.1 0.0 1.1 0.0 00.0 0.0 0.0
TENSOR epsname2 CONSTANT_ORTHOROT 1.1 0.0 1.1 0.0 1.1 0.0 00.0 0.0 0.0
TENSOR epsname3 CONSTANT_ORTHOROT 1.1 0.0 1.1 0.0 1.1 0.0 00.0 0.0 0.0
TENSOR muname1 CONSTANT_OVERGEN 1.0 -0.0 0.0 0.0 0.0 0.0 0.0 0.0 1.0 \
                                -0.0 0.0 0.0 0.0 0.0 0.0 0.0 1.0 -0.0
TENSOR xiname1 CONSTANT_OVERGEN 0.0 0.0 0.0 0.0 0.0 0.0 0.0 0.0 0.0 \
                                0.0 0.0 -0.0 0.0 0.0 0.0 0.0 0.0 0.0
TENSOR zetaname1 CONSTANT_OVERGEN 0.0 0.0 0.0 0.0 0.0 0.0 0.0 0.0 0.0 \
                                0.0 0.0 0.0 0.0 0.0 0.0 0.0 0.0 0.0

SURFACE 1 0.150250E+02 sigma1 sigma2
SURFACE 2 0.252412E+02 sigma1 sigma2
SURFACE 3 0.332320E+02 sigma1 sigma2
SURFACE 4 45.0 sigma1 sigma2
SIGMATYPE sigma1 1 1.0e+08 0.0
SIGMATYPE sigma2 1 0.00 0.0

```

Note that the optimum grid angles are approximately 15.0° , 25.2° , 33.3° and the pre-defined 45° . Plots showing the reflectivities and transmissivities in dB are given in figures 3-14 and 3-15. The frequency interval was chosen so that the end points of the interval did not strongly control the performance, and the results show an approximately equi-ripple \mathcal{R}_{22} as desired.

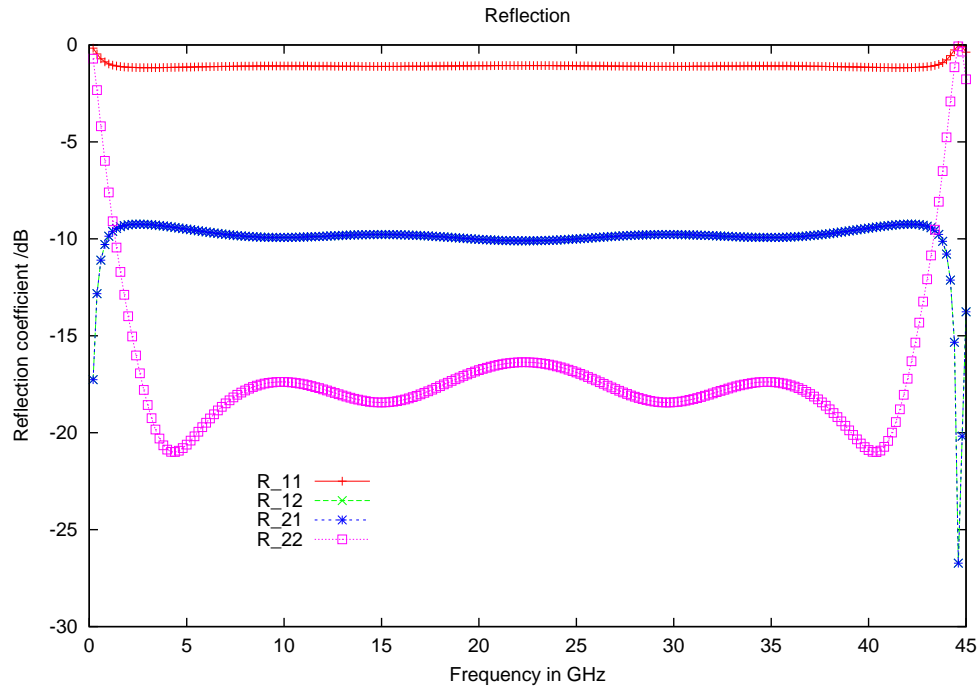


Figure 3-12: Reflection coefficients \mathcal{R}_{11} , \mathcal{R}_{12} , \mathcal{R}_{21} , \mathcal{R}_{22} in dB for example 7a.

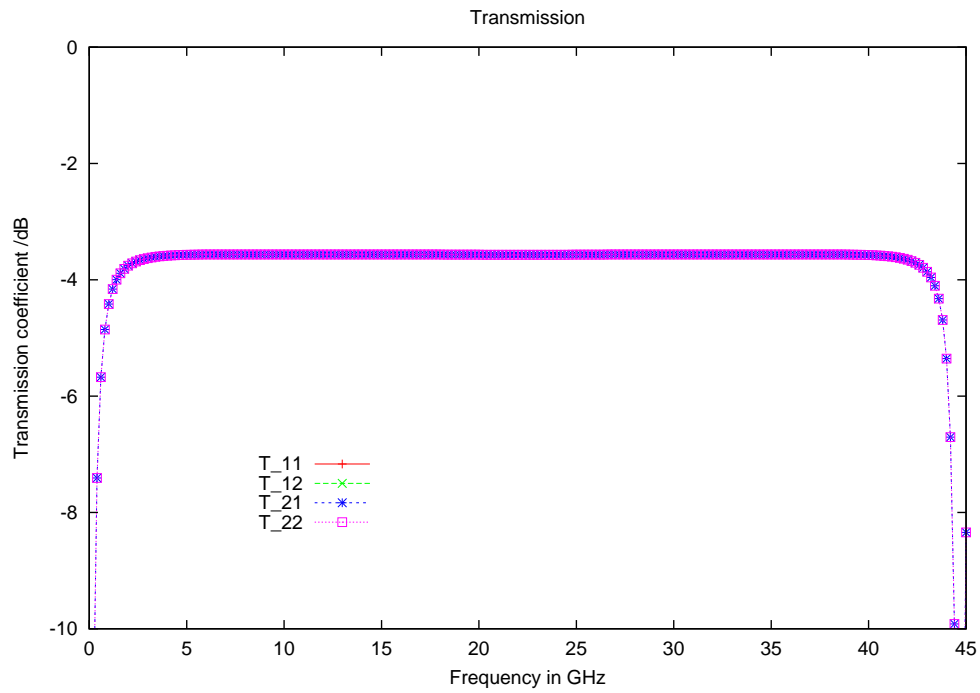


Figure 3-13: Transmission coefficients \mathcal{T}_{11} , \mathcal{T}_{12} , \mathcal{T}_{21} , \mathcal{T}_{22} in dB for example 7a.

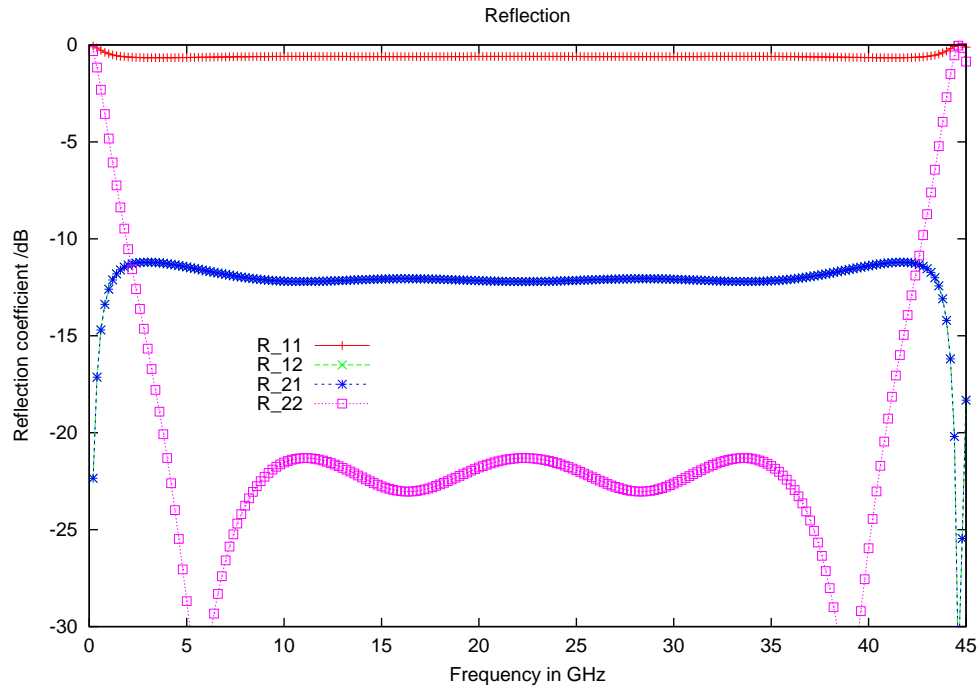


Figure 3-14: Reflection coefficients \mathcal{R}_{11} , \mathcal{R}_{12} , \mathcal{R}_{21} , \mathcal{R}_{22} in dB for example 7b.

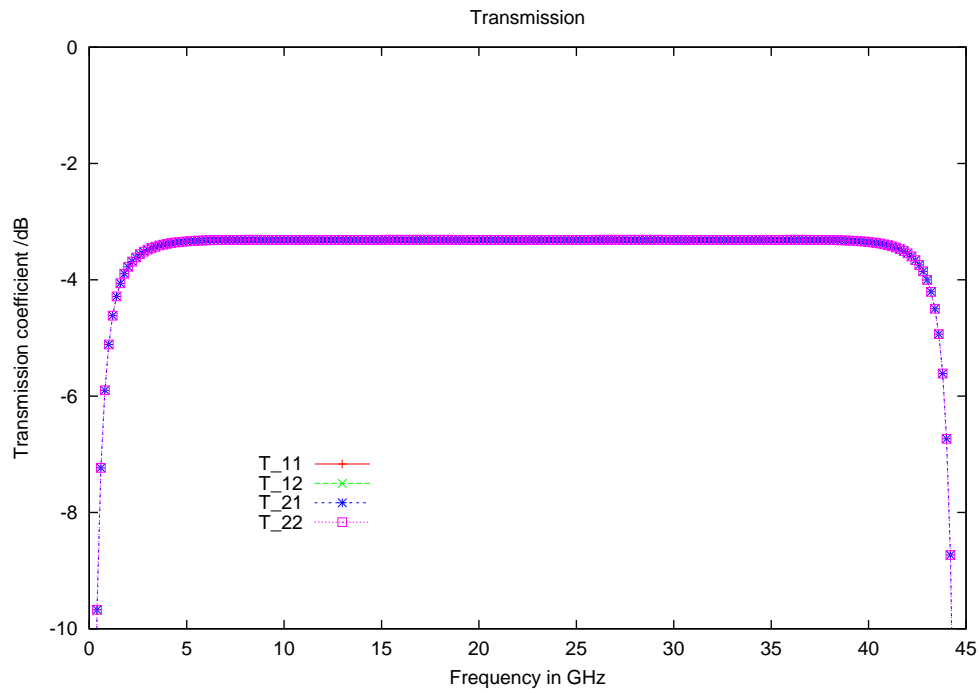


Figure 3-15: Transmission coefficients \mathcal{T}_{11} , \mathcal{T}_{12} , \mathcal{T}_{21} , \mathcal{T}_{22} in dB for example 7b.

4 References

- 1 *Sten Rikte, Gerhard Kristensson, Michael Andersson* “Propagation in bian-isotropic media - reflection and transmission ” Report CODEN:LUTEDX/(TEAT-7067)1-32/(1998), Lund Institute of Technology, Department of Electrosience, Sweden. (Available on web site <http://www.es.lth.se/teorel/Publications/TEAT-7000.../TEAT-7067.pdf>)
- 2 *Andrew Mackay* “The mathematical formulation of QDAS, Q-par Dichroic Array Software” Report Q-par/FSS/TRFSS2/1.1, Q-par Angus Ltd, UK, April 2003. (Available on web site <http://www.q-par.com>)
- 3 *Cleve Moler, Charles V. Loan* “Nineteen dubious ways to compute the exponential of a matrix, twenty-five years later” SIAM review, Vol. 45, No 1, pp1-46, February 2003 (Available on web site <http://www.cs.cornell.edu/cv/ResearchPDF/19ways+.pdf>)
- 4 *Roger B. Sidge* “EXPOKIT: Software package for computing matrix exponentials” Transactions on Mathematical Software (1998) (Documentation and source code available on web site <http://www.maths.uq.edu.au/expokit/>)
- 5 *W. V. T. Rusch, P. D. Potter* “Analysis of reflector antennas” Academic Press, 1970.
- 6 *W. H. Press, S. A. Teukolsky, W. T. Vetterling, B. P. Flannery* “Numerical recipes in Fortran 77” Cambridge university press, 1997.
- 7 *S. Pancharatnam* “Achromatic combinations of birefringent plates” memoir no. 71 of the Raman Research Institute, Bangalore, pp130-136. March 1955.
- 8 *L.D.Landau, E.M.Lifshitz* “Statistical Physics part 1”, Elsevier Press, 1980.
- 9 *L.D.Landau, E.M.Lifshitz, L.P.Pitaevski* “Electrodynamics of continuous media”, Elsevier Press, 1984.
- 10 *CST Computer simulation technology*. See web site www.cst.com.
- 11 *HFSS 3D Electromagnetic field simulation*. See web site www.ansoft.com.
- 12 *E. Anderson et al.* “LAPACK Users’ Guide, third edition, SIAM publishers. See also we site <http://www.netlib.org/lapack/lug>